第百七十二號

（昭和十四年一月發行）

抄　錄

螺旋渦により誘導される速度の計算及其のプロペラ理論への應用

所員　河　田　三　治

本論文は 1935～1937 年の間に著者が數回に亘り發表したる論文（本文序文註參照）を一篇にまとめ有限翼數としてプロペラの性能を分析するに便利ならしめ，併せてプロペラ後流の週期的流れの理論的解析を創めて試みたるものである．又二次元及軸對稱を有する三次元のポテンシァルのある流れに於けるが如く，螺旋渦による流れに於ても亦一種の流れの函數が定義されるものであることを示した．最後に理論からの結果は何れも實驗によつて確められることを示してある．

本研究の結論として次のことがわかつた．

1. プロペラ理論に於て翼の有限なることを考へに入れるのは，思つたより容易に行はれる．
2. これによる所謂先端効果はプロペラの外形等によつて著しく異るもので，場合によつては低ピッチに於ても $\left(\frac{v}{nD}=0.524\right)$ 14% にも達することがあるかと思へば，僅か 2% にすぎない場合もある．（第3章第2節）．一般に高ピッチのときは此の効果が大きい．
3. 單獨プロペラの性能は斯の如くして，翼素の性能から常に正確に計算出來る．
4. 後流の流れは週期的のものであるが，これも亦計算によつて求めることが出來る．

（終り）

This document is provided by JAXA.

No. 172.

(Published January, 1939.)

Calculation of Induced Velocity by Helical Vortices and Its Application to Propeller Theory.

By

Sandi KAWADA.

Member of the Institute.

Contents.

This document is provided by JAXA.

Introduction.

I have tried to arrange in order the papers[1] on the study of the velocity field induced by helical vortices and its applications, which I have published on various occasions during 1935–1937 and to develop a theory for the prediction of the propeller performance.

The vortex theory was a great success in its applications for aerofoils. The distribution of circulation and consequently the distribution of force along the span for a given aerofoil, its induced resistance, mutual interference between aerofoils or between aerofoil and boundary etc., were all brought within the reach of computation by its applications.

The vortex theory was also applied by some authors to elucidate the aerodynamic problems of the propellers. However, the success in this case was not so brilliant as in the case of aerofoils. The cause lies in that the calculation of the induced velocity by a finite number of helical vortices in a compact form was impossible and the authors were obliged to consider an hypothetical propeller with an infinite number of blades. In this case the induced velocity is given simply by

$$w_a = -p\omega\Gamma/4\pi v\,, \quad w_t = p\Gamma/4\pi r\,.$$

and it was found that the neighbouring elements of the blades can be treated as independent of each other. Therefore even at the tips of the blades there is no drop of circulation. This is evidently in contradiction with the experimental fact and this is the gravest defect of the simple vortex theory.

---

(1) "Induced Velocity by Helical Vortices,"
Journal of the Aeronautical Research Institute, Tokyo Imperial University, July, 1935 (In Japanese), Journal of the Aeronautical Sciences, Vol. 3, No. 3. Jan. 1936. etc.
"Effect of the Number of Blades on Propeller Characteristics," Journal of the Society of Aeronautical Science of Nippon, Dec, 1936 (In Japanese).
"On the Flow near the Propeller,"
Journal of the Society of Aeronautical Science of Nippon, July, 1937 (In Japanese).

This document is provided by JAXA.

I have obtained in Chapter I comparatively simple expressions for calculating the induced velocity by a finite number of helical vortices. In the following Chapters II and III the applications to the calculation of the performance of propeller are studied and in the last Chapter the theoretical considerations are verified by the experiment.

Chapter I. Theoretical Investigation.

1. *Induced Velocity by Helical Vortices.*

Take a propeller with p blades and consider the flow due to the free vortices shed from the tips and the centre. The free vortices shed from the intermediate positions are not considered. Thus this assumption is equivalent to assume a propeller with an uniform distribution of circulation along the radius.

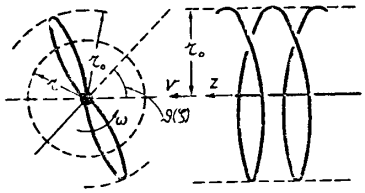

Fig. 1.

For the sake of simplicity the induced velocity is assumed to be small compared with the translational velocity of the propeller. The consideration is at first limited to the region remote from the propeller.

Let ω = angular velocity of the propeller,
v = translational velocity,
r, θ, z = semi-polar coordinates.

Then the equations to the surfaces described by the blades become[1]

$$\theta-\omega z/v = 0,\quad 2\pi/p,\quad \ldots\ldots,\quad 2(p-1)\pi/p.$$

If a new variable $\zeta = \theta-\omega z/v$ is introduced, the velocity potential due to the vortices becomes a function of r and ζ only. Furthermore we know that the potential must be a single valued function of the point and moreover it must be periodic in ζ with the period $2\pi/p$.[1]

(1) Goldstein, On the Vortex Theory of Screw Propellers, Proc. Roy. Soc., 123, 1929.

This document is provided by JAXA.

The Laplacian equation to be satisfied by the potential ϕ becomes

$$\frac{\partial^2\phi}{\partial r^2}+\frac{1}{r}\frac{\partial\phi}{\partial r}+\left(\frac{\omega^2}{v^2}+\frac{1}{r^2}\right)\frac{\partial^2\phi}{\partial\zeta^2}=0. \qquad (1)$$

Putting

$$\mu=\omega r/v$$

We have

$$\frac{\partial^2\phi}{\partial\mu^2}+\frac{1}{\mu}\frac{\partial\phi}{\partial\mu}+\left(1+\frac{1}{\mu^2}\right)\frac{\partial^2\phi}{\partial\zeta^2}=0. \qquad (2)$$

To obtain the solution of this equation it is convenient to consider outside and inside of the propeller wake separately.

Outside of the wake.

In this region the velocity potential must satisfy, besides the equation, the following boundary conditions:

ϕ, odd and periodic in ζ,

$\phi=0$ at $\mu=$ infinity.

We can construct the solution by taking an infinite series

$$\phi_0=\sum_{m=1}^{\infty}c_m(\mu)\sin pm\zeta. \qquad (3)$$

Substituting in (2)

$$\frac{\partial^2 c_m}{\partial\mu^2}+\frac{1}{\mu}\frac{\partial c_m}{\partial\mu}-p^2m^2\left(1+\frac{1}{\mu^2}\right)c_m=0. \qquad (4)$$

The solution of this equation is evidently

$$c_m=a_mK_{pm}(pm\mu), \qquad (5)$$

where K_{pm} is the modified Bessel function of the second kind and a_m is constant to be still determined.

Hence the solution becomes

$$\phi_0=\sum_{m=1}^{\infty}a_mK_{pm}(pm\mu)\sin pm\zeta. \qquad (6)$$

This document is provided by JAXA.

Inside of the wake.

In this region ϕ must have a discontinuity at the surfaces described by the blades and its amount must be equal to the circulation Γ at the point. Consider further a region $0 \leqq \zeta \leqq 2\pi/p$, then the difference in ϕ at $\zeta = 0$ and $\zeta = 2\pi/p$ must be equal to the circulation Γ which is constant along the radius.

Besides, since there is a straight vortex at the centre $\frac{1}{r}\frac{\partial \phi}{\partial \zeta}$ must become infinite as $1/r$ at $r = 0$.

If we put

$$\phi_i = -\frac{p\Gamma}{2\pi}\left(\frac{\pi}{p} - \zeta\right) + \sum_{m=1}^{\infty} b_m I_{pm}(pm\mu) \sin pm\zeta , \qquad (7)$$

all the conditions are satisfied and (7) must be the required solution. In the above expressions I_{pm} is the modified Bessel function of the first kind and b_m is constant to be determind.

The constants a_m and b_m can be determined from the continuity of ϕ_0 and ϕ_i as well as $\frac{\partial \phi_0}{\partial r}$ and $\frac{\partial \phi_i}{\partial r}$ at $r = r_0$, the radius of the helical vortices.

Now in the region $0 < \zeta < 2\pi/p$ we have in Fourier series the following relation

$$\frac{p}{2}\left(\frac{\pi}{p} - \zeta\right) = \sum_{m=1}^{\infty} \frac{1}{m} \sin pm\zeta . \qquad (8)$$

Therefore equating ϕ_0 and ϕ_i at $\mu = \mu_0$

$$a_m K_{pm}(pm\mu_0) = -\frac{\Gamma}{\pi m} + b_m I_{pm}(pm\mu_0) ,$$

and equating $\frac{\partial \phi_0}{\partial r}$ and $\frac{\partial \phi_i}{\partial r}$

$$a_m K'_{pm}(pm\mu_0) = b_m I'_{pm}(pm\mu_0)$$

This document is provided by JAXA.

We have therefore

$$a_m = -\frac{\Gamma}{\pi m}\cdot\frac{I'_{pm}(pm\mu_0)}{I'_{pm}(pm\mu_0)K_{pm}(pm\mu_0)-I_{pm}(pm\mu_0)K'_{pm}(pm\mu_0)},$$

$$b_m = -\frac{\Gamma}{\pi m}\cdot\frac{K'_{pm}(pm\mu_0)}{I'_{pm}(pm\mu_0)K_{pm}(pm\mu_0)-I_{pm}(pm\mu_0)K'_{pm}(pm\mu_0)}.$$

While we have[1]

$$I'_{pm}(pm\mu_0)K_{pm}(pm\mu_0)-I_{pm}(pm\mu_0)K'_{pm}(pm\mu_0) = \frac{1}{pm\mu_0}.$$

Therefore

$$a_m = -\frac{p\mu_0\Gamma}{\pi}\cdot I'_{pm}(pm\mu_0),$$

$$b_m = -\frac{p\mu_0\Gamma}{\pi}\cdot K'_{pm}(pm\mu_0). \qquad (9)$$

The expressions for ϕ_0 and ϕ_i become

$$\phi_0 = -\frac{p\mu_0\Gamma}{\pi}\sum_{m=1}^{\infty} I'_{pm}(pm\mu_0)K_{pm}(pm\mu)\sin pm\zeta, \quad \mu \geqq \mu_0$$

$$\phi_i = -\frac{p\Gamma}{2\pi}\left(\frac{\pi}{p}-\zeta\right)-\frac{p\mu_0\Gamma}{\pi}\sum_{m=1}^{\infty} K'_{pm}(pm\mu_0)I_{pm}(pm\mu)\sin pm\zeta. \quad \mu \leqq \mu_0. \qquad (10)$$

Now let

w_t = tangential component of induced velocity at the blade element,

w_a = axial component,

w = resultant of the above two $= \sqrt{w_t^2+w_a^2}$.

(1) Watson, Theory of Bessel Functions, p. 80, formula (19).

This document is provided by JAXA.

Then we have

$$w_t = \frac{1}{2}\left(\frac{1}{r}\frac{\partial\phi}{\partial\theta}\right)_{\zeta=0} = \frac{1}{2}\left(\frac{1}{r}\frac{\partial\phi}{\partial\zeta}\right)_{\zeta=0},$$

$$w_a = \frac{1}{2}\left(\frac{\partial\phi}{\partial z}\right)_{\zeta=0} = \frac{1}{2}\left(\frac{\partial\phi}{\partial\zeta}\frac{\partial\zeta}{\partial z}\right)_{\zeta=0} = -\mu w_t,$$

$$w_{t_0} = -\frac{p^2\mu_0\Gamma}{2\pi r}\sum_{m=1}^{\infty} mI'_{pm}(pm\mu_0)K_{pm}(pm\mu),$$

$$w_{ti} = \frac{p\Gamma}{4\pi r}\left[1-2p\mu_0\sum_{m=1}^{\infty} mK'_{pm}(pm\mu_0)I_{pm}(pm\mu)\right], \tag{11}$$

$$w_{a_0} = \frac{p^2\omega\mu_0\Gamma}{2\pi v}\sum_{m=1}^{\infty} mI'_{pm}(pm\mu_0)K_{pm}(pm\mu),$$

$$w_{ai} = -\frac{p\omega\Gamma}{4\pi v}\left[1-2p\mu_0\sum_{m=1}^{\infty} mK'_{pm}(pm\mu_0)I_{pm}(pm\mu)\right].$$

These are the induced velocities by a propeller with uniform distribution of circulation and therefore the induced velocities by helical vortices at the tips of the propeller and a straight vortex at the centre whose strength is p times that of the vortices at the tips. Hence to obtain the induced velocities due to the helical vortices only, we must substract the indiced velocities due to the straight vortex at the centre.

Therefore the tangential induced velocity becomes

$$w_{t_0} = -\frac{p\Gamma}{4\pi r}\left[1+2p\mu_0\sum_{m=1}^{\infty} mI'_{pm}(pm\mu_0)K_{pm}(pm\mu)\right],$$

$$w_{ti} = -\frac{p^2\mu_0\Gamma}{2\pi r}\sum_{m=1}^{\infty} mK'_{pm}(pm\mu_0)I_{pm}(pm\mu). \tag{12}$$

On the contrary the axial induced velocity is not influenced by the straight vortex and the expressions remain unchanged.

This document is provided by JAXA.

Thus,

$$w_{a_0} = \frac{p^2\omega\mu_0\Gamma}{2\pi v}\sum_{m=1}^{\infty} mI'_{pm}(pm\mu_0)K_{pm}(pm\mu)\,,$$

$$w_{ai} = -\frac{p\omega\Gamma}{4\pi v}\Big[1 - 2p\mu_0\sum_{m=1}^{\infty} m\,K'_{pm}(pm\mu_0)I_{pm}(pm\mu)\Big]\,. \qquad (13)$$

Thus we have obtained the induced velocities by a finite number of helical vortices in a compact form. However for numerical calculation these formulae are not so simple as they appear. This is due to the want of so complete a table of Bessel functions K_{pm} and I_{pm} as is required in the calculation. Fortunately, however, in most of the practical applications μ is fairly large and we can obtain an approximate values in the following way.

According to Nicholson[1] I_{pm} and K_{pm} are given by the following expressions for large values of order and argument.

---

(1) Nicholson, Phil. Mag. 1910.

To see the degree of approximation of this formula, take $p = 2$, $m = 1$, $\mu = 2$. The formula (14) gives

$$I_2(4) = 6{\cdot}3080\,,$$
$$K_2(4) = 0{\cdot}0177\,,$$

while the exact values are from table

$$I_2(4) = 6{\cdot}42219\,,$$
$$K_2(4) = 0{\cdot}01740\,,$$

The ratios become 0·9822 and 1·018 respectively.

In the actual propeller the free vortices springing from the blades are generally concentrated at the tips and near the boss.

The value of μ at the tip of the propeller is not usually smaller than 2 and the portion of the blades where the effect of the tip vortices are mostly felt are restricted to the region near the tips where μ is rarely smaller than 2 as before mentioned. Near the boss μ is very small and the formula ceases to be valid. But fortunately the contribution towards thrust and torque of this portion is very small. Considering this and remembering that the discussion are directed towards the first term in the series and that the error in the second and the higher terms rapidly tends to zero, the above simple formula seems to be quite sufficient for practical applications.

This document is provided by JAXA.

$$I_{pm}(pm\mu) = \left[\frac{1}{2\pi pm\sqrt{1+\mu^2}}\right]^{\frac{1}{2}} e^{pm\left\{\sqrt{1+\mu^2}-\frac{1}{2}\log_e\frac{\sqrt{1+\mu^2}+1}{\sqrt{1+\mu^2}-1}\right\}},$$

(14)

$$K_{pm}(pm\mu) = \left[\frac{\pi}{2pm\sqrt{1+\mu^2}}\right]^{\frac{1}{2}} e^{-pm\left\{\sqrt{1+\mu^2}-\frac{1}{2}\log_e\frac{\sqrt{1+\mu^2}+1}{\sqrt{1+\mu^2}-1}\right\}}.$$

We have then

$$I_{pm}(pm\mu)K_{pm}(pm\mu) = \frac{1}{2pm\sqrt{1+\mu^2}} \tag{15}$$

Differentiating with respect to $pm\mu$

$$I'_{pm}K_{pm}+I_{pm}K'_{pm} = -\frac{1}{2p^2m^2\mu^2}\left(1+\frac{1}{\mu^2}\right)^{-\frac{3}{2}}. \tag{16}$$

On the other hand we have as before

$$I'_{pm}K_{pm}-I_{pm}K'_{pm} = \frac{1}{pm\mu}.$$

Therefore

$$I'_{pm}K_{pm} = \frac{1}{2pm\mu}\left[1-\frac{1}{2pm\mu}\left(1+\frac{1}{\mu^2}\right)^{-\frac{3}{2}}\right]. \tag{17}$$

Similary

$$I_{pm}K'_{pm} = -\frac{1}{2pm\mu}\left[1+\frac{1}{2pm\mu}\left(1+\frac{1}{\mu^2}\right)^{-\frac{3}{2}}\right]. \tag{18}$$

And

$$\frac{K_{pm}(pm\mu)}{K_{pm}(pm\mu_0)} = \left[\frac{1+\mu_0^2}{1+\mu^2}\right]^{\frac{1}{4}} e^{-pmt_1},$$

$$\frac{I_{pm}(pm\mu)}{I_{pm}(pm\mu_0)} = \left[\frac{1+\mu_0^2}{1+\mu^2}\right]^{\frac{1}{4}} e^{-pmt_2}.$$

This document is provided by JAXA.

Therefore (11) becomes

$$w_{t_0} = -\frac{p\Gamma}{4\pi r}\left(\frac{1+\mu_0^2}{1+\mu^2}\right)^{\frac{1}{4}}\sum_{m=1}^{\infty}\left[1-\frac{1}{2pm\mu_0}\left(1+\frac{1}{\mu_0^2}\right)^{-\frac{3}{2}}\right]e^{-pmt_1},$$

$$w_{ti} = \frac{p\Gamma}{4\pi r}\left[1+\left(\frac{1+\mu_0^2}{1+\mu^2}\right)^{\frac{1}{4}}\sum_{m=1}^{\infty}\left\{1+\frac{1}{2pm\mu_0}\left(1+\frac{1}{\mu_0^2}\right)^{-\frac{3}{2}}\right\}e^{-pmt_2}\right], \tag{19}$$

or performing the summation

$$w_{t_0} = -\frac{p\Gamma}{4\pi r}\left(\frac{1+\mu_0^2}{1+\mu^2}\right)^{\frac{1}{4}}\left[\frac{1}{e^{pt_1}-1}-\frac{1}{2p\mu_0}\left(1+\frac{1}{\mu_0^2}\right)^{-\frac{3}{2}}\log_e\frac{1}{1-e^{-pt_1}}\right],$$

$$w_{ti} = \frac{p\Gamma}{4\pi r}\left[1+\left(\frac{1+\mu_0^2}{1+\mu^2}\right)^{\frac{1}{4}}\left\{\frac{1}{e^{pt_2}-1}+\frac{1}{2p\mu_0}\left(1+\frac{1}{\mu_0^2}\right)^{-\frac{3}{2}}\log_e\frac{1}{1-e^{-pt_2}}\right\}\right]. \tag{20}$$

where

$$t_1 = \sqrt{1+\mu^2}-\sqrt{1+\mu_0^2}-\frac{1}{2}\log_e\frac{(\sqrt{1+\mu^2}+1)(\sqrt{1+\mu_0^2}-1)}{(\sqrt{1+\mu^2}-1)(\sqrt{1+\mu_0^2}+1)}, \quad \mu \geqq \mu_0$$

$$t_2 = \sqrt{1+\mu_0^2}-\sqrt{1+\mu^2}+\frac{1}{2}\log_e\frac{(\sqrt{1+\mu^2}+1)(\sqrt{1+\mu_0^2}-1)}{(\sqrt{1+\mu^2}-1)(\sqrt{1+\mu_0^2}+1)}. \quad \mu \leqq \mu_0$$

In this form the calculation of the induced velocity is simple and easy.

2. *Discussions of the Expressions.*

The mean value of the induced velocities along the circumference is calculated from (10) as follows

$$(w_{t_0})_{\text{mean}} = \frac{1}{4\pi}\int_0^{2\pi}\frac{1}{r}\frac{\partial\phi_0}{\partial\zeta}d\zeta = 0,$$

$$(w_{ti})_{\text{mean}} = \frac{1}{4\pi}\int_0^{2\pi}\frac{1}{r}\frac{\partial\phi_i}{\partial\zeta}d\zeta = \frac{p\Gamma}{4\pi r}, \tag{21}$$

This document is provided by JAXA.

$$(w_{a_0})_{\text{mean}} = 0\,,$$

$$(w_{ai})_{\text{mean}} = -\frac{p\omega\Gamma}{4\pi v}\,.$$

Thus the mean value of the induced velocities depends only upon the circulation at the radius in consideration. Further we must notice that the expressions are just the same as those given in the simple vortex theory.

When the number of blades p or μ_0 is infinite we have

$$w_{t_0} = 0\,, \quad w_{ti} = \frac{p\Gamma}{4\pi r}\,, \quad w_{a_0} = 0\,, \quad w_{ai} = -\frac{p\omega\Gamma}{4\pi v}\,.$$

This is the case assumed in the simple vortex theory.

In the other extreme case $\omega = 0$, the helical vortices become straight and the tangential induced velocity must be given by[1]

$$\begin{aligned} w_{t_0} &= -\frac{p\Gamma}{4\pi r}\cdot\frac{r_0^p}{r^p - r_0^p}\,, \\ w_{ti} &= \frac{p\Gamma}{4\pi r}\left\{1 + \frac{p^p}{r_0^p - r^p}\right\}\,. \end{aligned} \tag{22}$$

Now from (12) we have when μ_0 and μ are very small, taking the predominent term in the expansions of I_{pm} and K_{pm}

$$I_{pm}(pm\mu) = \frac{\left(\frac{1}{2}pm\mu\right)^{pm}}{(pm)!}\,,$$

$$K_{pm}(pm\mu) = \frac{(pm-1)!}{2}\left(\frac{2}{pm\mu}\right)^{pm}\,,$$

$$I'_{nm}(pm\mu) = \frac{1}{2}(I_{pm-1} + I_{pm+1})$$

$$= \frac{1}{2}\frac{\left(\frac{pm\mu}{2}\right)^{pm-1}}{(pm-1)!}\,,$$

(1) W. Müller, Mathematische Strömungslehre, p. 97.

This document is provided by JAXA.

$$K'_{pm}(pm\mu) = -\frac{1}{2}(K_{pm-1}+K_{pm+1}) = -\frac{(pm)!}{4}\left(\frac{2}{pm\mu}\right)^{pm+1}.$$

Therefore

$$pm\mu_0 I'_{pm}(pm\mu_0)K_{pm}(pm\mu) = \frac{1}{2}\left(\frac{\mu_0}{\mu}\right)^{pm} = \frac{1}{2}\left(\frac{r_0}{r}\right)^{pm},$$

$$pm\mu_0 K'_{pm}(pm\mu_0)I_{pm}(pm\mu) = -\frac{1}{2}\left(\frac{\mu}{\mu_0}\right)^{pm} = -\frac{1}{2}\left(\frac{r}{r_0}\right)^{pm}, \tag{23}$$

$$w_{ti} = \frac{p\Gamma}{4\pi r}\left[1+\sum_{m=1}^{\infty}\left(\frac{r}{r_0}\right)^{pm}\right] = \frac{p\Gamma}{4\pi r}\left[1+\frac{r^p}{r_0^p-r^p}\right],$$

$$w_{t0} = -\frac{p\Gamma}{4\pi r}\sum_{m=1}^{\infty}\left(\frac{r_0}{r_0}\right)^{pm} = -\frac{p\Gamma}{4\pi r}\cdot\frac{r_0^p}{r^p-r_0^p}.$$

Thus we have obtained the expected results.

3. *Stream Function.*

As in the case of two dimensional flow or three dimensional flow with axial symmetry, we can define the stream function in the following way.

Take a small portion as in Fig. 2 whose three faces are parallel to $r =$ const., $z =$ const. and $\theta =$ const. Then the quantity of flow in this portion should be equal to that out of it in the same time.

From the face $(r+dr/2)d\vartheta dz$ a quantity of fluid equal to

$$\rho(r+dr/2)\left(w_r+\frac{1}{2}\frac{\partial w_r}{\partial r}dr\right)d\vartheta dz,$$

flows out and from the face $(r-dr/2)d\vartheta dz$ a quantity

$$\rho(r-dr/2)\left(w_r-\frac{1}{2}\frac{\partial w_r}{\partial r}dr\right)d\vartheta dz,$$

flows into this portion in unit of time.

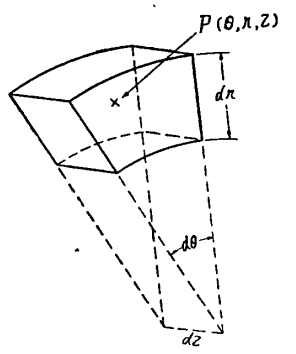

Fig. 2.

This document is provided by JAXA.

The difference becomes

$$-\rho\left(w_r+r\frac{\partial w_r}{\partial r}\right)dr\,d\vartheta\,dz=-\frac{\partial(rw_r)}{\partial r}\rho dr\,d\vartheta\,dz\,. \tag{24}$$

In the similar manner the excess of quantity of fluid flowing into the same portion from the faces parallel to $z=$ const. is

$$-\frac{\partial w_a}{\partial z}\rho r\,dr\,d\vartheta\,dz\,, \tag{25}$$

and the excess of quantity of fluid from the other faces becomes

$$-\frac{\partial w_t}{\partial \vartheta}\rho dr\,d\vartheta\,dz\,. \tag{26}$$

Therefore the condition that there should be no accumulation of the fluid requires

$$\frac{\partial(rw_r)}{\partial r}+r\frac{\partial w_a}{\partial z}+\frac{\partial w_t}{\partial \theta}=0\,.$$

We have from (11)

$$w_a=-\mu w_t\,,\qquad \zeta=\vartheta-\frac{\omega z}{v}\,.$$

Therefore

$$\frac{\partial w_a}{\partial z}=-\frac{\partial(\mu w_t)}{\partial \zeta}\frac{\partial \zeta}{\partial z}=\frac{\omega}{v}\mu\frac{\partial w_t}{\partial \zeta}\,,$$

$$\frac{\partial w_t}{\partial \theta}=\frac{\partial w_t}{\partial \zeta}\frac{\partial \zeta}{\partial \vartheta}=\frac{\partial w_t}{\partial \zeta}\,.$$

Hence it becomes

$$\frac{\partial(rw_r)}{\partial r}+\mu^2\frac{\partial w_t}{\partial \zeta}+\frac{\partial w_t}{\partial \zeta}=0\,,$$

or

$$\frac{\partial(rw_r)}{\partial r}+(\mu^2+1)\frac{\partial w_t}{\partial \zeta}=0\,. \tag{27}$$

This document is provided by JAXA.

This is the condition that w_r and w_t can be put in the form

$$w_r = -\frac{1}{r}\frac{\partial\psi}{\partial\zeta}, \qquad w_t = \frac{1}{1+\mu^2}\frac{\partial\psi}{\partial r}. \tag{28}$$

We can name ψ as stream function.

The equation for stream line is

$$\frac{dr}{w_r} = \frac{rd\vartheta}{w_t} = \frac{dz}{w_a}. \tag{29}$$

Since

$$\zeta = \vartheta - \frac{\omega}{v}z, \qquad d\zeta = d\vartheta - \frac{\omega}{v}dz,$$

from (29) we have

$$\frac{dr}{w_r} = \frac{d\vartheta - \frac{\omega}{v}dz}{w_t/r - \frac{\omega}{v}w_a} = \frac{rd\zeta}{(1+\mu^2)w_t}.$$

Putting ψ in this we have

$$\frac{dr}{-\frac{1}{r}\frac{\partial\psi}{\partial\zeta}} = \frac{rd\zeta}{\frac{\partial\psi}{\partial r}},$$

or

$$\frac{\partial\psi}{\partial r}dr + \frac{\partial\psi}{\partial\zeta}d\zeta = 0, \quad \text{or} \quad d\psi = 0. \tag{30}$$

Thus $\psi = \text{const.}$ represents a stream line.

The expression of the stream function can be easily obtained from that of the potential function as follows:

Since

$$\frac{1}{r}\frac{\partial\psi_0}{\partial\zeta} = -w_r = -\frac{\partial\phi_0}{\partial r} = \frac{p^2\mu_0\Gamma\frac{\omega}{v}}{\pi}\sum_{m=1}^{\infty} mI'_{pm}(pm\mu_0)K'_{pm}(pm\mu)\sin pm\zeta,$$

This document is provided by JAXA.

we have

$$\psi_0 = -\frac{p\mu\mu_0\Gamma}{\pi}\sum_{m=1}^{\infty} I'_{pm}(pm\mu_0)K'_{pm}(pm\mu)\cos pm\zeta + f_0(r)\,. \qquad (31)$$

Similarly

$$\psi_i = -\frac{p\mu\mu_0\Gamma}{\pi}\sum_{m=1}^{\infty} K'_{pm}(pm\mu_0)I'_{pm}(pm\mu)\cos pm\zeta + f_i(r)\,, \qquad (32)$$

where f_0 and f_i are arbitrary functions of r which will be determined as follows

$$\frac{\partial\psi_0}{\partial r} = -\frac{p^2\mu_0\Gamma\frac{\omega}{v}}{\pi}\sum_{m=1}^{\infty} I'_{pm}(pm\mu_0)\frac{\partial}{\partial\mu}\{\mu K'_{pm}(pm\mu)\}\cos pm\zeta + \frac{\partial f_0}{\partial r}$$

$$= -\frac{p^2\mu_0(1+\mu^2)\Gamma}{\pi r}\sum_{m=1}^{\infty} mI'_{pm}(pm\mu_0)K_{pm}(pm\mu)\cos pm\zeta + \frac{\partial f_0}{\partial r}\,.^{(1)} \qquad (33)$$

On the other hand

$$\frac{\partial\psi_0}{\partial r} = (1+\mu^2)w_t = \frac{1+\mu^2}{r}\frac{\partial\phi_0}{\partial\zeta}$$

$$= -\frac{p^2\mu_0(1+\mu^2)\Gamma}{\pi r}\sum_{m=1}^{\infty} mI'_{pm}(pm\mu_0)K_{pm}(pm\mu)\cos pm\zeta\,. \qquad (34)$$

Therefore f_0 becomes purely a constant.

Similarly

$$\frac{\partial\psi_i}{\partial r} = -\frac{p\mu_0\Gamma\frac{\omega}{v}}{\pi}\sum_{m=1}^{\infty} K'_{pm}(pm\mu_0)\frac{\partial}{\partial\mu}\{\mu I'_{pm}(pm\mu)\}\cos pm\zeta + \frac{\partial f_i}{\partial r}$$

$$= -\frac{p^2\mu_0(1+\mu^2)\Gamma}{\pi}\sum_{m=1}^{\infty} mK'_{pm}(pm\mu_0)I_{pm}(pm\mu)\cos pm\zeta + \frac{\partial f_i}{\partial r}\,. \qquad (35)$$

(1) The following relation is evident from the property of Bessel Functions.

$$\frac{\partial}{\partial\mu}\{\mu K'_{pm}(pm\mu)\} = pm\left(\mu+\frac{1}{\mu}\right)K_{pm}(pm\mu)\,.$$

This document is provided by JAXA.

On the other hand

$$\frac{\partial \psi_i}{\partial r} = \frac{1+\mu^2}{r}\frac{\partial \phi_i}{\partial \zeta}$$

$$= \frac{p(1+\mu^2)\Gamma}{2\pi r}\left[1 - 2p\mu_0 \sum_{m=1}^{\infty} mK'_{pm}(pm\mu_0)I_{pm}(pm\mu)\cos pm\zeta\right]. \tag{36}$$

Equating (35) and (36) we have

$$\frac{\partial f_i}{\partial r} = \frac{p\Gamma(1+\mu^2)}{2\pi r},$$

$$f_i = \frac{p\Gamma}{2\pi}\left\{\log_e \mu + \frac{1}{2}\mu^2\right\} + \text{const.} \tag{37}$$

Therefore the complete expression of the stream function becomes choosing f_0 so as to obtain the continuity of ψ_0 and ψ_i at $\mu = \mu_0$[1]

$$\psi_0 = \frac{p\Gamma}{2\pi}\left[\log_e \mu_0 + \frac{1}{2}\mu_0^2 - 2\mu\mu_0 \sum_{m=1}^{\infty} I'_{pm}(pm\mu_0)K'_{pm}(pm\mu)\cos pm\zeta\right],$$

$$\mu > \mu_0$$

$$\psi_i = \frac{p\Gamma}{2\pi}\left[\log_e \mu + \frac{1}{2}\mu^2 - 2\mu\mu_0 \sum_{m=1}^{\infty} K'_{pm}(pm\mu_0)I'_{pm}(pm\mu)\cos pm\zeta\right].$$

$$\mu < \mu_0 \tag{38}$$

---

(1) Now $\frac{1}{r}\frac{\partial \varphi}{\partial \zeta} = w_t = \frac{1}{1+\mu^2}\frac{\partial \psi}{\partial r}$, $\frac{\partial \varphi}{\partial r} = w_r = -\frac{1}{r}\frac{\partial \psi}{\partial \zeta}$,

$$\therefore \quad \frac{\partial \varphi}{\partial \zeta \partial r} = \frac{r}{1+\mu^2}\frac{\partial^2 \psi}{\partial r^2} + \frac{\partial \varphi}{\partial r}\frac{1-\mu^2}{(1+\mu^2)^2},$$

And $$\frac{\partial \varphi}{\partial r \partial \zeta} = -\frac{1}{r}\frac{\partial \psi}{\partial \zeta^2},$$

Equating we have the following equation which the stream function satisfies.

$$\frac{r}{1+\mu^2}\frac{\partial^2 \psi}{\partial r^2} + \frac{\partial \psi}{\partial r}\frac{1-\mu^2}{(1+\mu^2)^2} + \frac{1}{r}\frac{\partial^2 \psi}{\partial \zeta^2} = 0,$$

or $$\frac{\partial^2 \psi}{\partial \mu^2} + \frac{1}{\mu}\frac{1-\mu^2}{1+\mu^2}\frac{\partial \psi}{\partial \mu} + \left(1+\frac{1}{\mu^2}\right)\frac{\partial^2 \psi}{\partial \zeta^2} = 0.$$

This document is provided by JAXA.

4. *Calculation of the Stream Lines and the Comparison with the Experiment.*

From (38) we can easily calculate the stream lines. To lighten the labour in calculation the Nicholson's asymptotic expansion (14) was further simplified supposing μ^2 is large compared with the unity. The calculation was done for the case $\mu_0 = 6$. Fig. 3 shows the stream lines relative to the plane surface perpendicular to the axis of the helix and Fig. 4 shows them taken relative to the plane parallel to it. The figures affixed to the stream lines represents the value of $2\pi\psi / \Gamma\mu_0$.

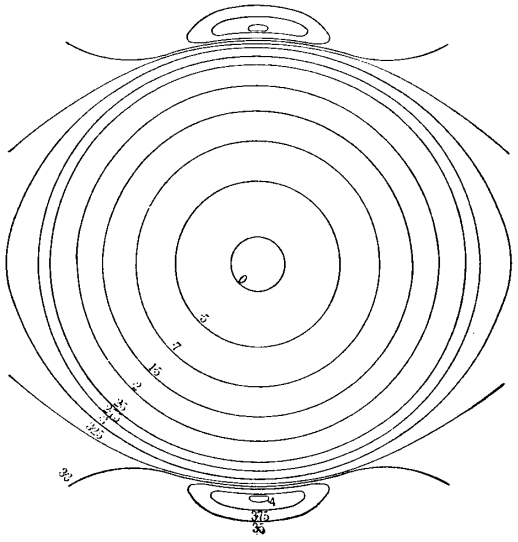

Fig. 3.

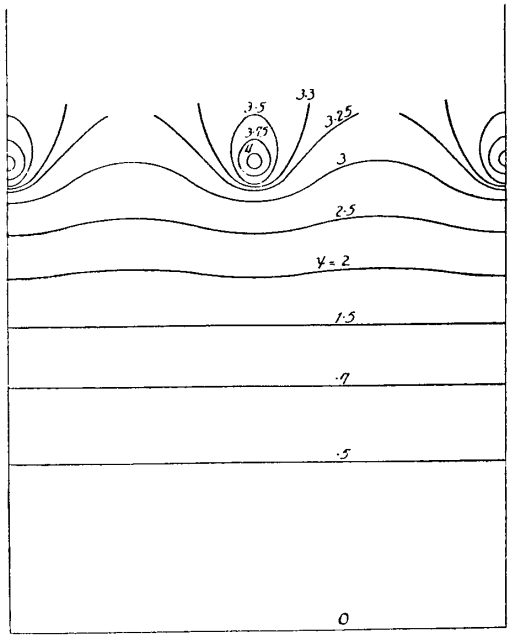

Fig. 4.

To obtain the stream lines experimentally, two methods were tried.

In the first method the hydrodynamical and electrical analogy was used. Cupper bars 4·5 mm in diameter were bent in the form of regular helix of 10 cm in diameter of $\mu_0 = 6$ and the direct current of about 100 amperes was sent through them as shown in Fig. 5.

The equipotential lines were made visible by scattering the iron dust on the plane placed

This document is provided by JAXA.

perpendicular and parallel to the axis of the helix. Fig. 6 and 7 show the obtained equipotential lines. We see that they are qualitatively in

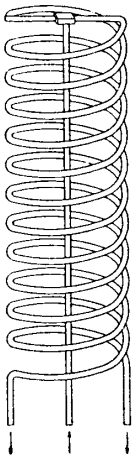

Fig. 5.

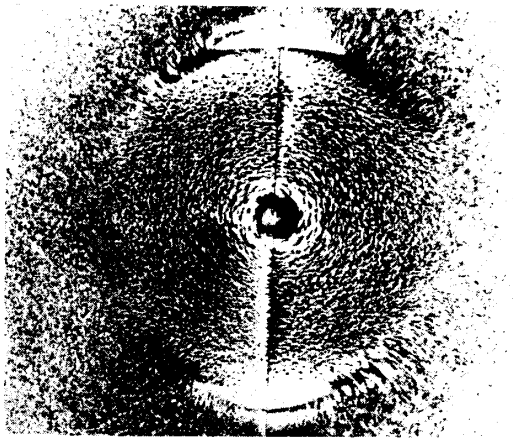

Fig. 6.

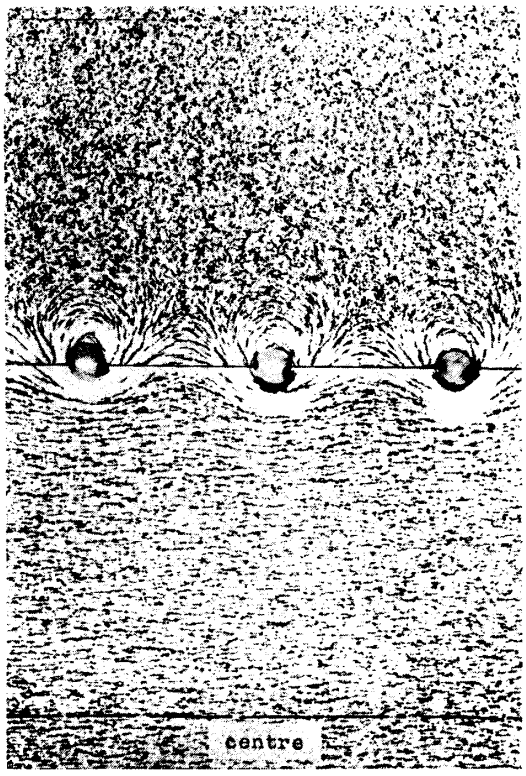

Fig. 7.

good agreement with the calculated stream lines. The behaviour of the equipotential lines near the helical conducting bars are somewhat different from the theoretical stream lines. This is due to the finite dimension of the bars. This distorts the equipotential lines close to the helical bars to a large extent owing to the severe obliquity of these to the plane perpendicular to the axis of the helix. The equipotential lines on the plane parallel to the axis are influenced in a much lesser degree as can be seen from Fig. 7.

In the second method the stream lines relative to the tank

This document is provided by JAXA.

(absolute stream lines) were photographed when the model propeller (23 cm in diameter) was moved through the water. Fig. 8 to Fig. 10 show the results of the experiment. The sheet of light, 1 cm in thickness, was shifted to 3 positions parallel to the axis. Therefore the photographs show the cross section of the stream lines at respective positions explained in the figures. In these experiment the value of μ_0 of tip vortices as revealed from Fig. 8 was approximately 3·8. The general behaviour of the tip vortices are well predicted by the theory.

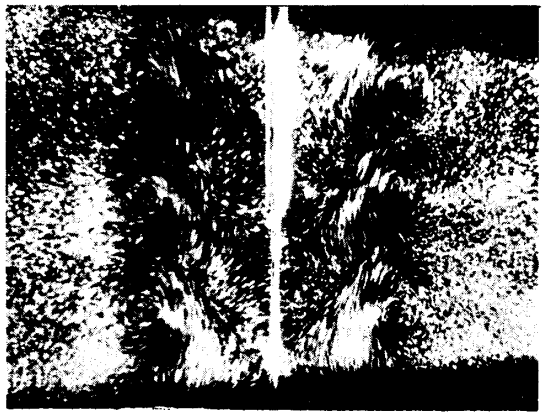

Fig. 8. Section containing the axis of rotation.

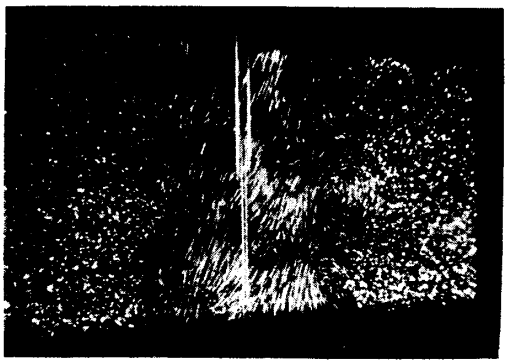

Fig. 9. Section at an half radius apart.

Chapter II. Method of Practical Applications.

1. *Extension to Arbitrary Distribution of Circulation.*

Thus far we have obtained the induced velocity by a propeller with an uniform distribution of circulation. When we are requested, in general, to calculate the induced velocity by a propeller with any distribution of circulation, an artifice to divide the propeller radius into as many divisions as possible in which the circulation is supposed constant and to apply the formulae above obtained is most convenient.

For example, let us divide the radius from $r = 0$ to $r = R$

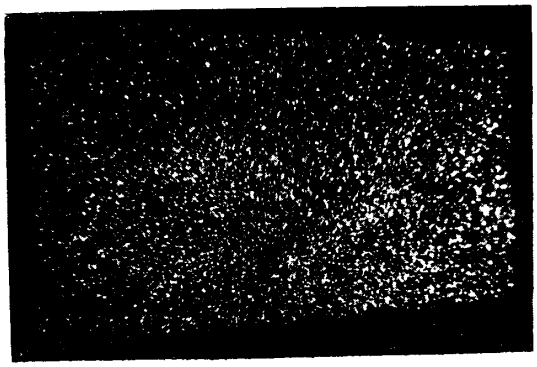

Fig. 10. Section outside of the propeller wash.

This document is provided by JAXA.

into eight divisions: $r = 0$ to $r = 0{\cdot}1R$, $r = 0{\cdot}1R$ to $r = 0{\cdot}3R$, $r = 0{\cdot}3R$ to $r = 0{\cdot}5R$, etc. as shown in Fig. 11 and let us suppose that in these divisions the values of the circulation is constant, being equal to the values at the centre of the divisions $r = 0{\cdot}05R$, $0{\cdot}2R$, etc.

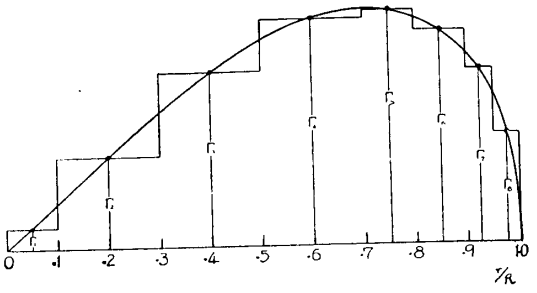

Fig. 11.

Then we have 9 sets of helical vortices at $r = 0$. $r = 0{\cdot}1\,R$, etc. and their respective circulations are Γ_1, $\Gamma_1-\Gamma_2$, $\Gamma_2-\Gamma_3$, ..., Γ_8.

Therefore the tangential induced velocity by these vortices is given by the following expression at $r = r_m$.

$$w_{tm} = \frac{pI_1}{4\pi r_m} + \frac{p(\Gamma_1-\Gamma_2)}{4\pi r_m}\lambda_{1m} + \frac{p(\Gamma_2-\Gamma_3)}{4\pi r_m}\lambda_{2m} + \ldots. + \frac{p\Gamma_8}{4\pi r_m}\lambda_{8m}$$

$$= \frac{p}{4\pi r_m}\left[\Gamma_1(1+\lambda_{1m}) - \Gamma_2(\lambda_{1m}-\lambda_{2m}) - \ldots. - \Gamma_8(\lambda_{7m}-\lambda_{8m})\right], \quad (39)$$

where

$$\lambda_{nm} = -1 - \left(\frac{1+\mu_{0m}^2}{1+\mu_m^2}\right)^{\frac{1}{4}}\left[\frac{1}{e^{pt_1}-1} - \frac{1}{2p\mu_{0n}}\left(1+\frac{1}{\mu_{0n}^2}\right)^{-\frac{3}{2}}\log_e\frac{1}{1-e^{-pt_1}}\right],$$

$$m > n$$

$$= \left(\frac{1+\mu_{0m}^2}{1+\mu_m^2}\right)^{\frac{1}{4}}\left[\frac{1}{e^{pt_2}-1} + \frac{1}{2p\mu_{0n}}\left(1+\frac{1}{\mu_{0n}^2}\right)^{-\frac{3}{2}}\log_e\frac{1}{1-e^{-pt_2}}\right].$$

$$m \leqq n.$$

t_1 and t_2 have same meaning as in (20).

2. *Calculation of Circulation for a Given Propeller.*

The problem which we encounter in the practice is to find out the distribution of circulation for a given propeller.

This document is provided by JAXA.

Before entering into the detail, it is essential to make an hypothesis upon which the propeller theory is to be based. Following the usual practice we make here the following assumptions:

1. Each element of the propeller blade is considered as an aerofoil in two dimensions.

2. Relative velocity of the air to the aerofoil is determined from the velocity of advance, number of rotation and the induced velocity at the element.

In this circumstance the circulation is given by

$$\begin{aligned} \Gamma &= k\pi t V \sin(\alpha - w/V) \\ &\fallingdotseq k\pi t V(\alpha - w/V) . \end{aligned} \tag{40}$$

where k = constant depending upon the aerofoil characteristics, being equal to unity for a thin aerofoil from the theory.

t = width of the element,

V = resultant velocity $= \sqrt{v^2 + \omega^2 r^2}$

w = resultant induced velocity,

α = apparent angle of incidence of the element counted from no-lift angle.

Then we have

$$w/V = \alpha - \Gamma/k\pi t V .$$

But since $w = w_t\sqrt{1+\mu^2}$,

$$V = v\sqrt{1+\mu^2},$$

we have

$$w_t/v = \alpha - \Gamma/k\pi t v\sqrt{1+\mu^2} .$$

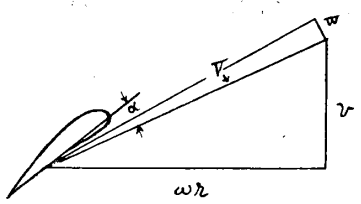

Fig. 12.

Putting in (39)

$$a_m v - \frac{\Gamma_m}{k_m \pi t_m \sqrt{1+\mu_m^2}} = \frac{p}{4\pi r_m}\left[(1+\lambda_{1m})\Gamma_1 - \cdots\cdots (\lambda_{7m} - \lambda_{8m})\Gamma_8\right] .$$

where $m = 1, \ldots, 8$.

This document is provided by JAXA.

Let

$$J_m = \frac{p\Gamma_m}{4\pi v R}, \qquad \beta_m = \frac{4r_m}{pk_m t_m \sqrt{1+\mu_m^2}}.$$

Then we have

$$(1+\lambda_{1m})J_1-(\lambda_{1m}-\lambda_{2m})J_2-\cdots\cdots-\{\lambda_{(m-1)m}-\lambda_{mm}-\beta_m\}J_m-\cdots\cdots$$
$$\cdots\cdots-(\lambda_{7m}-\lambda_{8m})J_8 = a_m\frac{r_m}{R}, \qquad (41)$$

where m should be taken to be 1, 2, ..., 8.

These equations can still be written in the form:

$$-a_{1m}J_1-a_{2m}J_2-\cdots\cdots+a_{mm}J_m-\cdots\cdots-a_{8m}J_8 = a_m\frac{r_m}{R}, \qquad (42)$$

where

$$a_{1m} = -(1+\lambda_{1m}),\ a_{2m} = \lambda_{1m}-\lambda_{2m},\ \cdots\cdots,\ a_{mm} = -(\lambda_{(m-1)m}-\lambda_{mm}-\beta_m),$$
$$\cdots\cdots,\ a_{8m} = \lambda_{7m}-\lambda_{8m}.$$

In these equations the coefficient $a_{nm}\,(n \neq m)$ are functions of $\mu_m = \omega r_m/v$ and $\mu_{0n} = \omega r_{0n}/v$ only and can be calculated from the formulae (39).

The coefficient β_m and the right hand side of the equations are depending upon the given characteristics of the propeller only.

The author calculated in Table 1 the coefficients a_{nm} for $\omega R/v = 3, 6$ and 9 by the formulae (39) and the values corresponding to $\omega R/v = 0$ $(\omega = 0)$ by the exact formulae:

$$\lambda_{nm} = -1-\frac{r_m^2}{r_m^2-r_{0n}^2}, \qquad m > n$$
$$= \frac{r_m^2}{r_{0n}^2-r_m^2}. \qquad m \leqq n \qquad (43)$$

The calculation was limited to the case $p = 2$. The values of coefficients for another values of μ_0 can be easily obtained from the interpolation. The coefficients β_m is depending principally upon the width of the element and the right hand side depends upon the shape of the propeller and must be calculated for each respective case.

This document is provided by JAXA.

TABLE I.

Values of the Coefficients a_{nm} (1).

1st eqn.		$\mu_0 = 0$	3	6	9
Coeff. of	J_1	1·33	1·36	1·31	1·28
	J_2	0·30	0·34	0·30	0·28
	J_3	0·03	0 01	0·01	0
	J_4	0	0	0	0
2nd eqn.	J_1	0·33	0·25	0·15	0·08
	J_2	2·13	1·91	1·53	1·28
	J_3	0·61	0·55	0 35	0·19
	J_4	0·11	0·08	0·03	0·01
	J_5	0·02	0·01	0	
	J_6	0·02	0·01	0	
	J_7	0·01	0		
3rd eqn.	J_1	0·07	0·03	0·01	0
	J_2	1·21	0·64	0·28	0·15
	J_3	4·06	2·70	1·74	1·37
	J_4	1·30	0·85	0·42	0·21
	J_5	0·16	0 09	0·02	0·01
	J_6	0·08	0·04	0·01	0
	J_7	0·03	0·01	0	
	J_8	0·03	0·01	0	
4th eqn. Coeff. of	J_1	0·03	0·01	0	
	J_2	0·30	0·07	0·01	0
	J_3	2·44	0·76	0·34	0·17
	J_4	6·04	3·01	1·81	1·38
	J_5	1·48	0·74	0·35	0·18
	J_6	0 49	0·23	0·08	0·02
	J_7	0·13	0·05	0·02	0·01
	J_8	0·11	0·05	0	0

(1) When $n = m$, the value of $a_{nm} - \beta_m$ is given in the Table.

This document is provided by JAXA.

TABLE I.—(*Continued*).

		$\mu_0 = 0$	3	6	9
5th eqn.	J_1	0·02	0		
	J_2	0·17	0·03	0	
	J_3	0·61	0·14	0·04	0·01
	J_4	6·00	2·21	1·06	0·63
	J_5	15·0	6·15	3·35	2·35
	J_6	4·93	2·07	1·03	0·63
	J_7	0·61	0·25	0·11	0·05
	J_8	0·38	0·15	0·05	0·01
6th eqn.	J_1	0·01	0		
	J_2	0·13	0·01	0	
	J_3	0·39	0·07	0·01	0
	J_4	1·58	0·43	0·15	0·06
	J_5	6·09	1·95	0·95	0·59
	J_6	17·0	6·27	3·36	2·36
	J_7	4·14	1·58	0·79	0·50
	J_8	1·36	0·52	0·25	0·13
7th eqn. Coeff. of	J_1	0·01	0		
	J_2	0·11	0·01	0	
	J_3	0·29	0·03	0	
	J_4	0·83	0·21	0·06	0·01
	J_5	1·72	0·46	0·19	0·09
	J_6	13·64	4·84	2·46	1·59
	J_7	38·05	12·57	6·61	4·49
	J_8	13·51	4·25	2·18	1·43
8th eqn.	J_1	0·01	0		
	J_2	0·09	0·01	0	
	J_3	0·25	0·02	0	
	J_4	0·71	0·13	0·03	0·01
	J_5	0·99	0·25	0·09	0·03
	J_6	3·72	1·10	0·50	0·28
	J_7	12·22	4·09	2·12	1·38
	J_8	38·0	12·64	6·64	4·49

This document is provided by JAXA.

3. *Solution of the Equations and the Investigation of the Applicability of the Method.*

As an example suppose a propeller with constant width, constant apparent angle of incidence and uniform blade section throughout, the circulation of which is related by

$$\Gamma = \pi t V(a - w/V), \qquad \text{as before.}$$

Suppose $\mu_0 = 3$, $p = 2$, $pt/R = 0{\cdot}3$. We have then

TABLE 2.

r/R	β_m	r/R	β_m
0·05	0·66	0·75	4·06
0·2	2·29	0·85	4·14
0·4	3·41	0·925	4·18
0·6	3·88	0·975	4·21

The equations become putting now $J = p\Gamma/4\pi vRa$.

$$\begin{aligned}
2{\cdot}02J_1 - 0{\cdot}34J_2 - 0{\cdot}01J_3 &= 0{\cdot}05,\\
-0{\cdot}25J_1 + 4{\cdot}20J_2 - 0{\cdot}55J_3 - 0{\cdot}08J_4 - 0{\cdot}01J_5 - 0{\cdot}01J_6 &= 0{\cdot}2,\\
-0{\cdot}03J_1 - 0{\cdot}64J_2 + 6{\cdot}11J_3 - 0{\cdot}85J_4 - 0{\cdot}09J_5 - 0{\cdot}04J_6 - 0{\cdot}01J_7 & \\
- 0{\cdot}01J_8 &= 0{\cdot}4,\\
-0{\cdot}01J_1 - 0{\cdot}07J_2 - 0{\cdot}76J_3 + 6{\cdot}89J_4 - 0{\cdot}74J_5 - 0{\cdot}23J_6 - 0{\cdot}05J_7 & \\
- 0{\cdot}05J_8 &= 0{\cdot}6,\\
-0{\cdot}03J_2 - 0{\cdot}14J_3 - 2{\cdot}21J_4 + 10{\cdot}21J_5 - 2{\cdot}07J_6 - 0{\cdot}25J_7 & \\
- 0{\cdot}15J_8 &= 0{\cdot}75,\\
-0{\cdot}01J_2 - 0{\cdot}07J_3 - 0{\cdot}43J_4 - 1{\cdot}95J_5 + 10{\cdot}41J_6 - 1{\cdot}58J_7 & \\
- 0{\cdot}52J_8 &= 0{\cdot}85,\\
-0{\cdot}01J_2 - 0{\cdot}03J_3 - 0{\cdot}21J_4 - 0{\cdot}46J_5 - 4{\cdot}84J_6 + 16{\cdot}75J_7 & \\
- 4{\cdot}25J_8 &= 925,\\
-0{\cdot}01J_2 - 0{\cdot}02J_3 - 0{\cdot}13J_4 - 0{\cdot}25J_5 - 1{\cdot}10J_6 - 4{\cdot}09J_7 & \\
+ 16{\cdot}85J_8 &= 0{\cdot}975. \qquad (44)
\end{aligned}$$

This document is provided by JAXA.

It is not an easy task to solve these simultaneous equations in an ordinary manner. However the present equations permit us to obtain the solution by successive approximation.

In the first place obtain the approximate values of J. The simple vortex theory gives these approximate values. In this theory it is thought

$$\lambda_{1m}, \lambda_{2m}, \cdots = 0, \lambda_{mm} = 1, \lambda_{m,1}, \cdots = 0.$$

Therefore the first approximate values of J become

$$J_1 = 0.030,\ J_2 = 0.061,\ J_3 = 0.091,\ J_4 = 0.123,\ J_5 = 0.148,$$
$$J_6 = 0.165,\ J_7 = 0.179,\ J_8 = 0.187.$$

Now put $J_2, J_3, \ldots$ above obtained in the first of the equations; $J_1, J_3, \ldots$ in the second; and so forth.

We have thus the second approximation. Repeating this process several times we obtain finally the required solution. This is shown in Table 3.

TABLE 3.

	J_1	J_2	J_3	J_4	J_5	J_6	J_7	J_8
1st appro.	0.030	0.061	0.091	0.123	0.148	0.165	0.179	0.187
2nd	0.032	0.064	0.093	0.122	0.145	0.152	0.156	0.115
3rd	0.036	0.065	„	0.121	0.135	0.144	0.134	0.109
4th	„	„	0.092	0.120	0.134	0.139	0.130	0.103
5th	„	„	„	0.119	0.133	0.137	0.126	0.102
6th	„	„	„	„	„	„	„	0.101
7th	„	„	„	„	„	0.136	„	„
8th	„	„	„	„	„	„	„	„

Thus if we take three significant figures the 8 repetitions of the calculation gives the exact solution and if we take two figures only 5 repetitions are sufficient. The length of the calculation depends upon

This document is provided by JAXA.

p and μ_0, becoming less complicated with increasing values of p and μ_0. At any rate the solution of the equations is not so laborious as it at first appears.

When the values of circulation are known, the induced velocities at the element can be calculated as follows. The relation between the tangential induced velocity w_t and the circulation is given, as before shown, by

$$w_t = av - \frac{\Gamma}{k\pi t\sqrt{1+\mu^2}}$$

$$= av\left\{1 - J\beta\frac{R}{r}\right\},$$

or

$$w_t/\omega_r = \frac{a}{\mu}\left\{1 - J\beta\frac{R}{r}\right\}, \quad w_a/v = a\mu\left\{1 - J\beta\frac{R}{r}\right\}. \qquad (45)$$

In Table 4 the values of $w_t/\omega r$ and w_a/v are calculated supposing $a = 0{\cdot}1$ radian. The values deduced from the simple vortex theory are shown in the same table. The induced velocities above calculated are those at the blade element. The mean value along the circumference of the induced velocities which we can measure directly in experiment and represented by

$$w_t = p\Gamma/4\pi r, \qquad w_a = p\omega\Gamma/4\pi v,$$

are also shown.

The applicability of the present method can be best studied by the comparison of the result with that obtained from the exact treatment of the problem. One of the cases which can be dealt with exactly is the one in which

$$\omega = 0, \qquad p = 1.$$

This document is provided by JAXA.

TABLE 4.

Present theory			Simple theory		Mean value	
r/R	$w_t/\omega r$	w_a/v	$w_t/\omega r$	w_a/v	$w_t/\omega r$	w_a/v
0·05	0·35	0·008	0·40	0·009	0·48	0·011
0·2	0·043	0·015	0·051	0·018	0·054	0·0195
0·4	0·018	0·026	0·019	0·027	0·019	0·028
0·6	0·013	0·041	0·011	0·037	0·011	0·036
0·75	0·012	0·063	0·009	0·044	0·008	0·040
0·85	0·013	0·086	0·008	0·050	0·006	0·041
0·925	0·0155	0·119	0·007	0·054	0·005	0·038
0·975	0·019	0·165	0·007	0·056	0·0035	0·030

In fact this corresponds to the case of an aerofoil in rectilinear motion. We can also infer that the interference velocity is largest in this case. Suppose that the aerofoil is a rectangular one in plan form and the cross section and the angle of incidence are uniform along the span. Let us calculate the circulation by the method mentioned before and let us compare the result with the exact one obtained directly. Take $k = 1$, aspect ratio 5. We have the equations:

$$\begin{aligned}
&9{\cdot}597J_1-2{\cdot}559J_2-0{\cdot}285J_3-0{\cdot}109J_4-0{\cdot}033J_5-0{\cdot}024J_6-0{\cdot}011J_7\\
&\qquad -0{\cdot}010J_8 = 1,\\
&-0{\cdot}799J_1+6{\cdot}381J_2-1{\cdot}066J_3-0{\cdot}213J_4-0{\cdot}053J_5-0{\cdot}038J_6-0{\cdot}016J_7\\
&\qquad -0{\cdot}013J_8 = 1,\\
&-0{\cdot}133J_1-1{\cdot}067J_2+6{\cdot}381J_3-1{\cdot}066J_4-0{\cdot}133J_5-0{\cdot}080J_6-0{\cdot}029J_7\\
&\qquad -0{\cdot}024J_8 = 1,\\
&-0{\cdot}053J_1-0{\cdot}213J_2-1{\cdot}066J_3+6{\cdot}381J_4-0{\cdot}799J_5-0{\cdot}267J_6-0{\cdot}070J_7\\
&\qquad -0{\cdot}058J_8 = 1,\\
&-0{\cdot}040J_1-0{\cdot}102J_2-0{\cdot}285J_3-2{\cdot}559J_4+9{\cdot}579J_5-2{\cdot}132J_6-0{\cdot}267J_7\\
&\qquad -0{\cdot}160J_8 = 1,\\
&-0{\cdot}024J_1-0{\cdot}078J_2-0{\cdot}166J_3-0{\cdot}609J_4-2{\cdot}132J_5+9{\cdot}579J_6-1{\cdot}599J_7\\
&\qquad -0{\cdot}532J_8 = 1,\\
&-0{\cdot}021J_1-0{\cdot}062J_2-0{\cdot}120J_3-0{\cdot}334J_4-0{\cdot}569J_5-5{\cdot}117J_6+15{\cdot}976J_7\\
&\qquad -4{\cdot}265J_8 = 1,\\
&-0{\cdot}018J_1-0{\cdot}054J_2-0{\cdot}099J_3-0{\cdot}246J_4-0{\cdot}331J_5-1{\cdot}218J_6-4{\cdot}265J_7\\
&\qquad +15{\cdot}976J_8 = 1, \qquad (46)
\end{aligned}$$

where $J = \dfrac{\Gamma}{4vab}$, b = half span.

This document is provided by JAXA.

The solution of this system of equations is

$J_1 = 0{\cdot}179$, $J_2 = 0{\cdot}233$, $J_3 = 0{\cdot}250$, $J_4 = 0{\cdot}250$, $J_5 = 0{\cdot}238$,
$J_6 = 0{\cdot}219$, $J_7 = 0{\cdot}187$, $J_8 = 0{\cdot}140$.

More accurate method of Glauert gives the following values shown in Table 5.

TABLE 5.

y/b	*J*
0	0·249
0·2588	0 246
0·50	0·234
0·7071	0·211
0·8660	0·169
0·9659	0·098

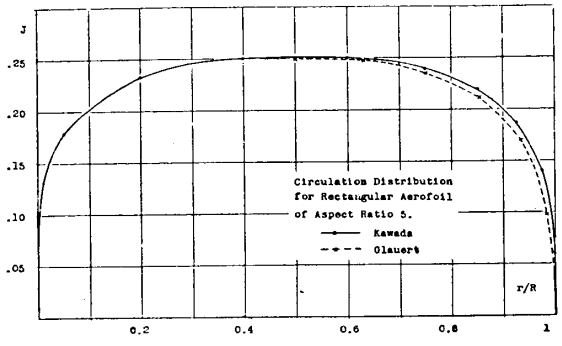

Fig. 13.

The results are compared in Fig. 13. We see that the coincidence is fairly good. The comparison also suggests that the increase of the number of divisions ameriolates the result.

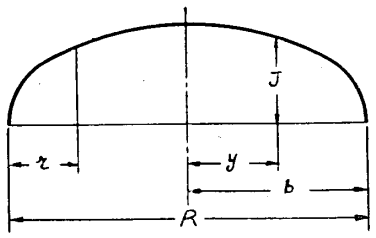

Fig. 14.

Considering that in the actual cases of propeller p is greater than 2 and ω is different from zero, we can safely conclude that the error introduced by the assumption of step by step distribution of circulation is always negligible and the method is well suited for the purpose.

CHAPTER III. APPLICATIONS TO PROPELLER THEORY.

1. *Expressions for Thrust and Torque.*

We could thus find out the values of circulation along the radius of the propeller. The expressions for thrust and torque can be written

This document is provided by JAXA.

down according to the hypothesis made in the preceeding chapter that the behaviour of an element of the blade is similar to that of a single aerofoil with the same cross section with the relative velocity composed of v and ωr, and that the force due to the circulation acts normally to the resultant of these two velocities, while the force due to the profile resistance acts in the direction of the resultant velocity. Therefore the thrust which is the component of force in the direction of v is

$$\frac{dT}{dr} = \rho p \Gamma(\omega r - w_t) - \text{force due to the profile resistance}$$

$$= \rho p \Gamma(\omega r - w_t) - \frac{1}{2} C_{xo} \rho p v^2 t \sqrt{1+\mu^2}\,. \qquad (47)$$

and the torque which is the component force in the direction of ωr multiplied by r is

$$\frac{dQ}{dr} = \rho p \Gamma r(v + w_a) + \text{torque due to the profile resistance}$$

$$= \rho p \Gamma r(v + w_a) + \frac{1}{2} C_{xo} \rho p t \omega r^2 v \sqrt{1+\mu^2}\,. \qquad (48)$$

where C_{xo} is the coefficient of the profile resistance of the blade element under consideration, ρ is the density of the fluid and t is the width of the element.

2. *Investigation of the Tip Effect.*

In order to investigate the tip effect, let us take out some typical propellers and let us calculate the distribution of circulation and thrust.

In all these examples the value of k is taken to be unity and the profile resistance was neglected. Moreover the induced velocity was supposed to be very small. All these resitrictions were introduced to simplify the calculations and it will be shown later that these restrictions can be easily removed if necessary.

This document is provided by JAXA.

Ex. 1. Constant width, constant angle of incidenee propeller.

$$\text{Solidity} = \sigma = pt/R = 0{\cdot}3\,, \quad \mu_0 = 6\,, \quad p = 2\,.$$

In this case the equations to determine Γ become

$$\begin{aligned}
1{\cdot}95J_1 - 0{\cdot}30J_2 - 0{\cdot}01J_3 &= 0{\cdot}05,\\
-0{\cdot}15J_1 + 3{\cdot}24J_2 - 0{\cdot}35J_3 - 0{\cdot}03J_4 &= 0{\cdot}20,\\
-0{\cdot}01J_1 - 0{\cdot}28J_2 + 3{\cdot}79J_3 - 0{\cdot}42J_4 - 0{\cdot}02J_5 - 0{\cdot}01J_6 &= 0{\cdot}40,\\
-0{\cdot}01J_2 - 0{\cdot}34J_3 + 3{\cdot}95J_4 - 0{\cdot}35J_5 - 0{\cdot}08J_6 - 0{\cdot}02J_7 &= 0{\cdot}60,\\
-0{\cdot}04J_3 - 1{\cdot}06J_4 + 5{\cdot}52J_5 - 1{\cdot}03J_6 - 0{\cdot}11J_7 - 0{\cdot}05J_8 &= 0{\cdot}75,\\
-0{\cdot}01J_3 - 0{\cdot}15J_4 - 0{\cdot}95J_5 + 5{\cdot}54J_6 - 0{\cdot}79J_7 - 0{\cdot}25J_8 &= 0{\cdot}85,\\
-0{\cdot}06J_4 - 0{\cdot}19J_5 - 2{\cdot}46J_6 + 8{\cdot}80J_7 - 2{\cdot}18J_8 &= 0{\cdot}925,\\
-0{\cdot}03J_4 - 0{\cdot}09J_5 - 0{\cdot}50J_6 - 2{\cdot}12J_7 + 8{\cdot}83J_8 &= 0{\cdot}975.
\end{aligned} \tag{49}$$

$$\text{where} \quad J = \frac{\Gamma}{2\pi v R a}\,.$$

Proceeding as it was explained previously and taking as the first approximation the circulation corresponding to infinite number of blades:

$$J_1 = 0{\cdot}031, \quad J_2 = 0{\cdot}0738, \quad J_3 = 0{\cdot}131, \quad J_4 = 0{\cdot}191, \quad J_5 = 0{\cdot}237,$$
$$J_6 = 0{\cdot}267, \quad J_7 = 0{\cdot}290, \quad J_9 = 0{\cdot}306.$$

we have finally the following values:

$$J_1 = 0{\cdot}039, \quad J_2 = 0{\cdot}080, \quad J_3 = 0{\cdot}134, \quad J_4 = 0{\cdot}189, \quad J_5 = 0{\cdot}223,$$
$$J_6 = 0{\cdot}237, \quad J_7 = 0{\cdot}222, \quad J_8 = 0{\cdot}180.$$

Now when $w_i/\omega r$ is small, the expression for thrust can be written

$$\frac{dT}{dr} = p\rho\Gamma\omega r$$

This document is provided by JAXA.

or

$$\frac{dC_T}{dr} = \frac{1}{\rho n^2 D^4}\frac{dT}{dr} = \frac{\pi^3 a}{\mu_0 R}\cdot\frac{r}{R}\cdot J$$

In Table 6 and in Fig. 15 the values of $\frac{R}{a}\frac{dC_T}{dr}$ are given as well as those deduced from the simple vortex theory which corresponds to the case of infinite number of blades of same solidity.

It may be seen that there is a marked difference in thrust near the tips and in other places the difference is small. This decrease of the thrust near the tip is the so-called "tip effect" of the propeller due to the finiteness of the number of blades.

TABLE 6.

Values of $\frac{R}{a}\frac{dC_T}{dr}$.

r/R	Present theory	Simple theory
0·05	0·003	0·002
0·2	0·021	0·019
0·4	0·067	0·067
0·6	0·15	0·15
0·75	0·21	0·23
0·85	0·26	0·30
0·925	0·26	0.35
0.975	0·23	0·39

Ex. 2. $p = 3$, the other conditions are same as in Ex. 1.

The equations to determine the circulation become

This document is provided by JAXA.

$$
\begin{aligned}
1{\cdot}77J_1-0{\cdot}13J_2 &= 0{\cdot}05,\\
-0{\cdot}05J_1+2{\cdot}92J_2-0{\cdot}13J_3 &= 0{\cdot}20,\\
-0{\cdot}13J_2+3{\cdot}38J_3-0{\cdot}20J_4 &= 0{\cdot}40,\\
-0{\cdot}15J_3+3{\cdot}50J_4-0{\cdot}18J_5-0{\cdot}03J_6 &= 0{\cdot}60,\\
-0{\cdot}01J_3-0{\cdot}60J_4+4{\cdot}48J_5-0{\cdot}62J_6-0{\cdot}05J_7-0{\cdot}02J_8 &= 0{\cdot}75,\\
-0{\cdot}06J_4-0{\cdot}56J_5+4{\cdot}51J_6-0{\cdot}50J_7-0{\cdot}13J_8 &= 0{\cdot}85,\\
-0{\cdot}01J_4-0{\cdot}09J_5-1{\cdot}55J_6+6{\cdot}58J_7-1{\cdot}37J_8 &= 0{\cdot}925,\\
-0{\cdot}01J_4-0{\cdot}03J_5-0{\cdot}28J_6-1{\cdot}30J_7+6{\cdot}60J_8 &= 0{\cdot}975.
\end{aligned}
\tag{50}
$$

where $J=\dfrac{3\Gamma}{4\pi vRa}$.

Since the solidity is the same as in Ex. 1, the simple vortex theory gives the same result as in Ex. 1. The solution of the equations gives the following result given in Table 7 and in Fig. 15.

TABLE 7.

Values of $\dfrac{R}{a}\dfrac{dC_T}{dr}$.

r/R	Present theory	Simple theory
0·05	0·002	0·002
0·2	0·019	0·019
0·4	0·067	0·067
0·6	0·15	0·15
0·75	0·22	0·23
0·85	0·27	0·30
0·925	0·295	0·35
0·975	0·26	0·39

This document is provided by JAXA.

Ex. 3. $p = 4$, and the other conditions remain unchanged.

The equations become

$$
\begin{aligned}
1{\cdot}69J_1 - 0{\cdot}052 &= 0{\cdot}05,\\
-0{\cdot}02J_1 + 2{\cdot}80J_2 - 0{\cdot}07J_3 &= 0{\cdot}20,\\
-0{\cdot}06J_2 + 3{\cdot}21J_3 - 0{\cdot}09J_4 &= 0{\cdot}40,\\
-0{\cdot}08J_3 + 3{\cdot}32J_4 - 0{\cdot}09J_5 - 0{\cdot}01J_6 &= 0{\cdot}60,\\
-0{\cdot}39J_4 + 3{\cdot}99J_5 - 0{\cdot}40J_6 - 0{\cdot}02J_7 - 0{\cdot}01J_8 &= 0{\cdot}75,\\
-0{\cdot}02J_4 - 0{\cdot}37J_5 + 4{\cdot}01J_6 - 0{\cdot}33J_7 - 0{\cdot}07J_8 &= 0{\cdot}85,\\
-0{\cdot}04J_5 - 1{\cdot}11J_6 + 5{\cdot}57J_7 - 1{\cdot}02J_8 &= 0{\cdot}925,\\
-0{\cdot}01J_5 - 0{\cdot}17J_6 - 0{\cdot}98J_7 + 5{\cdot}58J_8 &= 0{\cdot}975.
\end{aligned}
\qquad (51)
$$

and the solution of these equations give the result shown in Table 8 and in Fig. 15.

TABLE 8.

Values of $\dfrac{R}{a}\dfrac{dC_T}{dr}$.

r/R	$\dfrac{R}{\alpha}\dfrac{dC_T}{dr}$
0·05	0·002
0·2	0 019
0·4	0·067
0·6	0·15
0·75	0 22
0·85	0·285
0 925	0·31
0·975	0·285

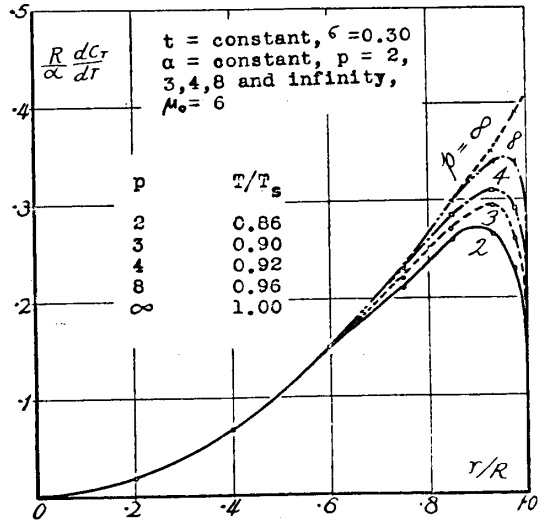

Fig. 15.

This document is provided by JAXA.

Ex. 4. $p = 8$, and the other conditions remain unchanged.

The equations become

$$\begin{aligned}
1{\cdot}64J_1 &= 0{\cdot}05,\\
2{\cdot}71J_2 &= 0{\cdot}20,\\
3{\cdot}06J_3 - 0{\cdot}01J_4 &= 0{\cdot}40,\\
-0{\cdot}01J_3 + 3{\cdot}15J_4 - 0{\cdot}01J_5 &= 0{\cdot}60,\\
-0{\cdot}09J_4 + 3{\cdot}36J_5 - 0{\cdot}10J_6 &= 0{\cdot}75,\\
-0{\cdot}09J_5 + 3{\cdot}37J_6 - 0{\cdot}09J_7 - 0{\cdot}01J_8 &= 0{\cdot}85,\\
-0{\cdot}40J_6 - 4{\cdot}03J_7 - 0{\cdot}41J_8 &= 0{\cdot}925,\\
-0{\cdot}03J_6 - 0{\cdot}38J_7 + 4{\cdot}03J_8 &= 0{\cdot}975.
\end{aligned} \tag{52}$$

and we have the result shown in Table 9 and in Fig. 15.

TABLE 9.

Values of $\frac{R}{\alpha}\frac{dC_T}{dr}$.

r/R	$\frac{R}{\alpha}\frac{dC_T}{dr}$	r/R	$\frac{R}{\alpha}\frac{dC_T}{dr}$
0·05	0·002	0·75	0·23
0·2	0·019	0 85	0·30
0·4	0·057	0·925	0·34
0·6	0·15	0·975	0·34

The reduction of the thrust in these cases is shown in Table 10, taking the thrust corresponding to the infinite number of blades to be unity.

TABLE 10.

p	2	3	4	8	infinity
Ratio of Thrust	0·86	0·90	0·92	0·96	1·00

Ex. 5. Now the solidity was doubled without changing the other conditions in Ex. 1., namely, constant width, constant angle of incidence, $\mu_0 = 6$, $\sigma = 0{\cdot}6$.

This document is provided by JAXA.

The result is shown in Table 11 and in Fig. 16. The ratio T/T_s decreased from 0·86 to 0·835, thus showing that the tip effect increases with the relative blade width.

TABLE 11

Values of $\frac{R}{a}\frac{dC_T}{dr}$.

r/R	Present theory	Simple theory
0·05	0·004	0·002
0·2	0·031	0·028
0·4	0·10	0·10
0·6	0·22	0·22
0·75	0·32	0·35
0·85	0·37	0·45
0·925	0·36	0·53
0·975	0·30	0·58

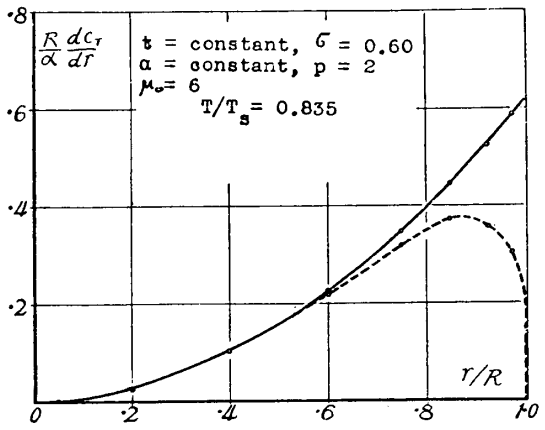

Fig. 16. Simple theory ———
Present theory - - - - - -

Ex. 6. Same as in Ex. 1. except $\mu_0 = 9$ instead of 6.

The result is shown in Table 12 and in Fig. 17. Together with the example mentioned before, namely the case where $\mu_0 = 3$, we can conclude that the tip effect decreases with the increase of μ_0.

TABLE 12.

Values of $\frac{R}{a}\frac{dC_T}{dr}$.

r/R	Present theory	Simple theory
0·05	0·002	0·001
0·2	0·02	0·02
0·4	0·06	0·06
0·6	0·13	0 13
0·75	0·19	0·20
0·85	0·24	0·25
0·925	0·25	0·30
0·975	0·22	0·33

The ratio T/T_s becomes 0·91.

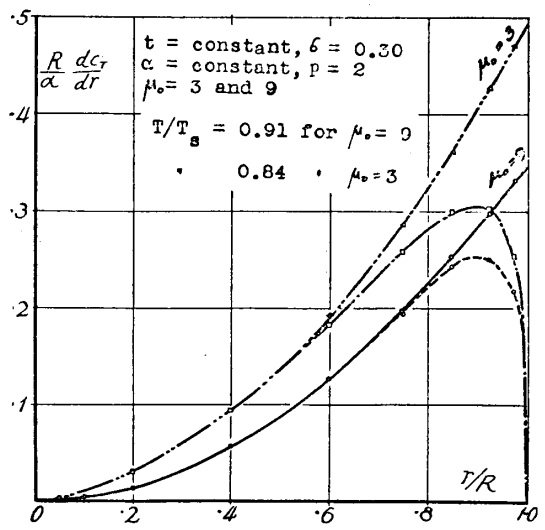

Fig. 17. Simple theory [- - —— - - ——
Present theory [—— · —— · ——
- - - - - - - -

This document is provided by JAXA.

Ex. 7. Constant angle of incidence propeller, $p = 2$, $\mu_0 = 6$, the width is tapered towards the tip:

$$t = t_0\left(1 - \frac{1}{2}r^2/R^2\right), \qquad \sigma = pt_0/R = 0{\cdot}6\,.$$

We have the result shown in Table 13 and in Fig. 18.

TABLE 13.

Values of $\dfrac{R}{a}\dfrac{dC_T}{dr}$.

r/R	Present theory	Simple theory
0·05	0·004	0·002
0·2	0·03	0·03
0·4	0·10	0·10
0·6	0·19	0·20
0·75	0·27	0·29
0·85	0·30	0·34
0·925	0·29	0·38
0·975	0·24	0·395

The ratio T/T_s becomes 0·88.

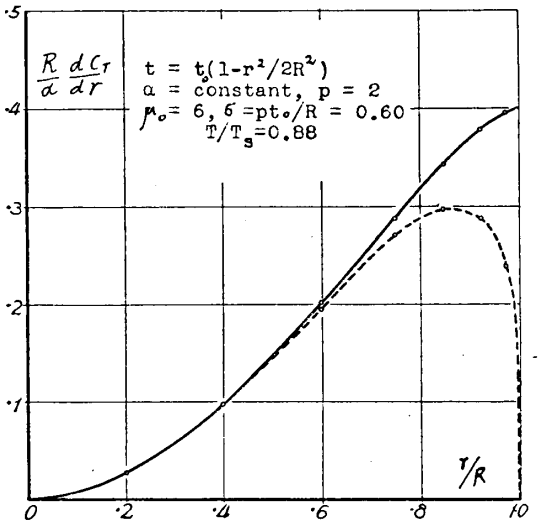

Fig. 18. Simple theory ———
Present theory - - - - -

Ex. 8. Constant width propeller, $\sigma = 0{\cdot}3$, $\mu_0 = 6$, $p = 2$ and $a = a_0(1 - r/R)$.

We have the result shown in Table 14 and in Fig. 19.

TABLE 14.

Values of $\dfrac{R}{a_0}\dfrac{dC_T}{dr}$.

r/R	Present theory	Simple theory
0·05	0·002	0·016
0·2	0·016	0·015
0·4	0·039	0·041
0·6	0·0565	0·059
0·75	0·054	0·057
0·85	0·042	0·044
0·925	0·027	0·026
0·975	0·014	0·010

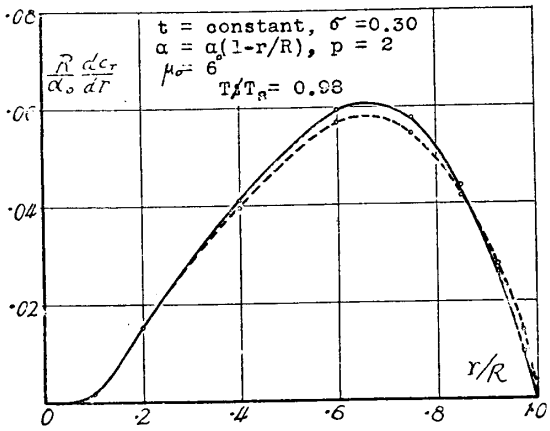

Fig. 19. Simple theory ———
Present theory - - - - - -

This document is provided by JAXA.

In this last example the value of T/T_s becomes 0·98. The simple vortex theory gives nearly the correct value and the tip effect is very small. Thus the tip effect of the propeller differs to a large extent according to the propeller and it is difficult to write down a general rule. But it may be said that the tip effect decreases with the increase in the number of blades and μ_0 for a given type of propeller. In the above examples the smallest tip effect was only 2 percent. This explains the reason why the prediction from the simple vortex theory, which does not take into consideration the tip losses, can afford in some cases quite a good result. It will also be made clear, that even if in some cases the simple vortex theory gives very good results, it is premature to conclude that it is the satisfactory theory.

3. *Investigation of the Periodic Flow behind the Propeller.*

It is thought that the flow behind the propeller is highly periodic in nature and there are some experimental explorations of flow. On the theoretical side, however, it was impossible till now to know even qualitatively the flow pattern behind the propeller.

The expressions for indueed velocity by helical vortices (10) permit us to calculate this periodic flow. For the sake of simplicity let us calculate the periodic flow induced at a radial distance r by the vortices shed at a single radius r_0.

Ex. 1. $\mu_0 = 6,\ r/r_0 = 0{\cdot}95,\ p = 2.$

In this case we have the following series to calculate the induced velocity w_t.

$$\begin{aligned} w_t/w_{tm} = 1 &+ 0{\cdot}584\cos 2\zeta + 0{\cdot}315\cos 4\zeta + 0{\cdot}172\cos 6\zeta + 0{\cdot}094\cos 8\zeta \\ &+ 0{\cdot}051\cos 10\zeta + 0{\cdot}028\cos 12\zeta + 0{\cdot}015\cos 14\zeta + 0{\cdot}008\cos 16\zeta \\ &+ 0{\cdot}005\cos 18\zeta + 0{\cdot}0025\cos 20\zeta + \cdots, \end{aligned} \tag{53}$$

where w_{tm} represents the mean value of the tangential induced velocity along the circumference and is equal to $p\Gamma/4\pi r$.

This document is provided by JAXA.

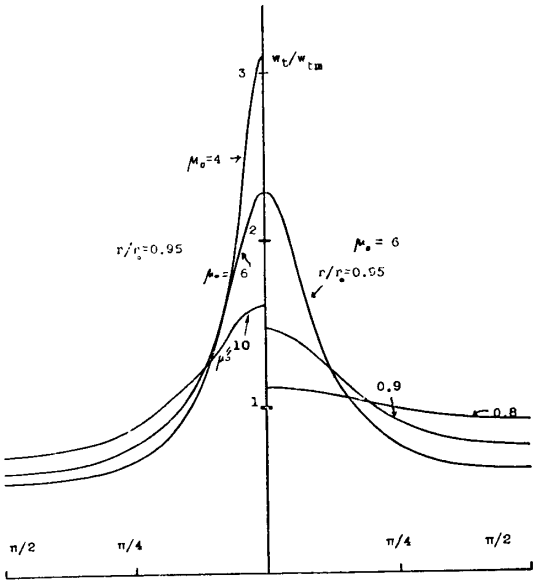

Fig. 20.

The axial induced velocity w_a can be calculated by the relation

$$w_a = -\mu w_t$$

The values of w_t/w_{tm} for some values of ζ are given in Table 15 and in Fig. 20.

Ex. 2. $\mu_0 = 6$, $r/r_0 = 0{\cdot}9$, $p = 2$.

We have

$$w_t/w_{tm} = 1 + 0{\cdot}314\cos 2\zeta + 0{\cdot}095\cos 4\zeta + 0{\cdot}029\cos 6\zeta + 0{\cdot}009\cos 8\zeta + 0{\cdot}003\cos 10\zeta + 0{\cdot}0007\cos 12\zeta + \cdots\cdots . \quad (54)$$

Ex. 3. $\mu_0 = 6$, $r/r_0 = 0{\cdot}8$, $p = 2$.

We have

$$w_t/w_{tm} = 1 + 0{\cdot}100\cos 2\zeta + 0{\cdot}009\cos 4\zeta + 0{\cdot}0007\cos 6\zeta + \cdots\cdots . \quad (55)$$

Ex. 4. $\mu_0 = 4$, $r/r_0 = 0{\cdot}95$, $p = 2$.

We have

$$w_t/w_{tm} = 1 + 0{\cdot}718\cos 2\zeta + 0{\cdot}465\cos 4\zeta + 0{\cdot}304\cos 6\zeta + 0{\cdot}200\cos 8\zeta + 0{\cdot}139\cos 10\zeta + 0{\cdot}093\cos 12\zeta + 0{\cdot}062\cos 14\zeta + 0{\cdot}042\cos 16\zeta + 0{\cdot}028\cos 18\zeta + 0{\cdot}017\cos 20\zeta + 0{\cdot}011\cos 22\zeta + 0{\cdot}008\cos 24\zeta + 0{\cdot}005\cos 26\zeta + 0{\cdot}003\cos 28\zeta + 0{\cdot}002\cos 30\zeta + \cdots\cdots . \quad (56)$$

Ex. 5. $\mu_0 = 10$, $r/r_0 = 0{\cdot}95$, $p = 2$.

We have

This document is provided by JAXA.

$$w_t/w_{tm} = 1 + 0\cdot387\cos 2\zeta + 0\cdot140\cos 4\zeta + 0\cdot051\cos 6\zeta + 0\cdot019\cos 8\zeta - 0\cdot007\cos 10\zeta + 0\cdot002\cos 12\zeta + 0\cdot001\cos 14\zeta + \cdots\cdots . \quad (57)$$

TABLE 15.

Values of w_t/w_{tm}.

Ex. / ζ_x	Ex. 1	Ex. 2	Ex. 3	Ex. 4	Ex. 5
0	2·28	1·47	1·11	3·10	1·61
$\pi/16$	1·76	1·38	—	1·86	1·47
$\pi/8$	1·18	1·20	1·07	1·09	1·21
$\pi/4$	0·76	0·90	0·99	0·67	0·88
$3\pi/8$	0·64	0·78	0·93	0·58	0·75
$\pi/2$	0·62	0·75	0·91	0·56	0·72

We see that the fluctuation in flow is largest near the vortex filaments and rapidly dies away with the distance from it and also that the fluctuation decreases with the increase in the value of μ_0. From this we can safely conclude that for actual propellers the fluctuation of flow is largest near the tips and for the high pitched propellers.

To compare with these results, deduced from purely theoretical considerations, the flow in the propeller wake was measured experimentally with a calibrated hot-wire direction and speed meter.(1) The experiments were carried out in 1·5 meters wind tunnel of the Institute

Fig. a.

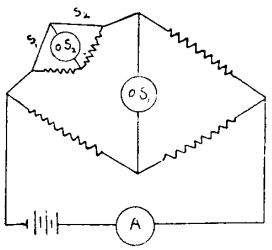

Fig. b. S_1, S_2 hot-wire.

(1) The hot-wire direction and speed meter is constructed from fine platinum wire (0·015 mm in diameter) span across three supports also of platinum wire (0·5 mm in diameter) as shown in the figure. The length of each branch of platinum wire is 6mm and the angle between them is 30°. The two branches of platinum wire were placed in double Wheatstone bridge as shown in the figure. The galvanometer OS_1 measures the speed fluctuation and OS_2 the direction of the wind. The meter was calibrated after each experiment. The propeller was driven by 1 HP electric motor placed under the wind tunnel by means of chain belt and the space behind the propeller was left unobstructed as far as possible.

This document is provided by JAXA.

using a two bladed propeller of 0·7 m. in diameter (see Fig. 21). To minimise the effect of inertia on the records of instantaneous velocity a very fine platinum wire 0·015 mm in diameter was employed together with very low translational speed of the propeller. For example, in experiment No. 37 the translational speed was 3·64 m/s and r.p.s. was 7·70.

Fig. 21.

The records are reproduced in Fig. 22 and the rotational induced velocity w_t was calculated from these records. The hot-wire was placed

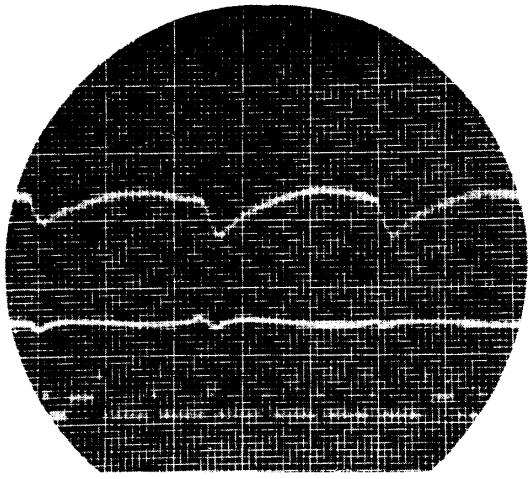

No. 37. Upper line shows the variation of direction, middle line the variation of speed and lower line time interval of 1/50 sec.

Fig. 22 (a).

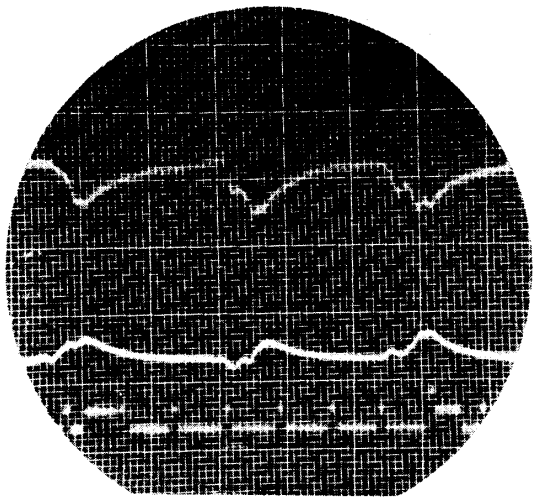

No. 41. Upper line shows the variation of direction, middle line the variation of speed and lower line time interval of 1/50 sec.

Fig. 22 (b).

at a distance of 6 times the diameter of the propeller. Therefore we can safely ignore the influence of the blades themselves. The record show that the induced velocity differs a bit according to one blade or other and also according to time. We picked up a record corresponding to one revolution of the propeller and analysed it.

To facilitate the comparison with the theoretical results we calculated from these results the quantity w_t/w_{tm}.

This document is provided by JAXA.

As zero point of the angular position the position when the hot-wire came just behind the trailing edge of the blade element was taken.

The results are shown in Fig. 23.

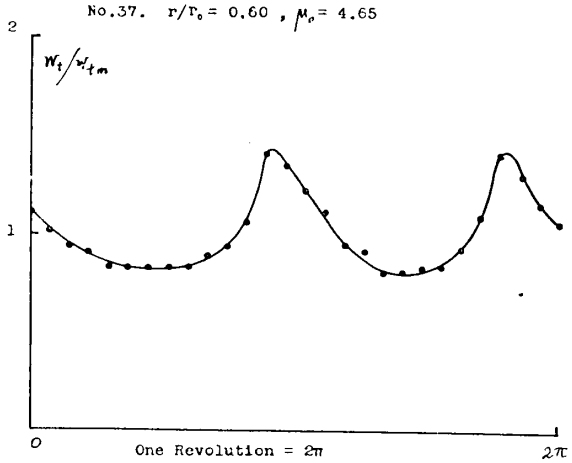

Fig. 23 (a).

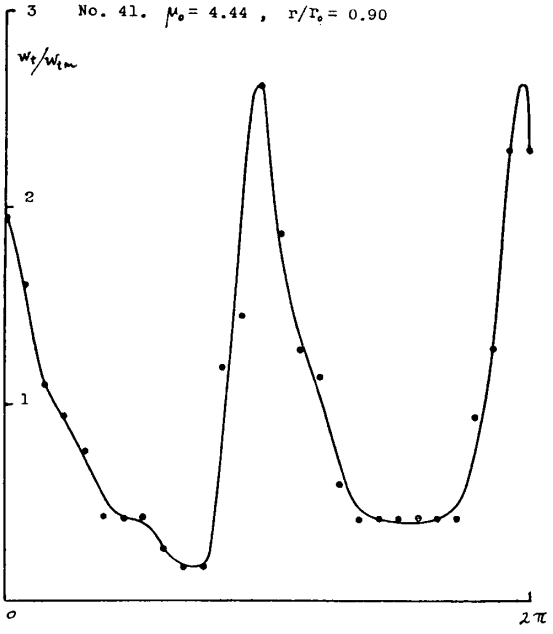

Fig. 23 (b).

The general behaviour of w_t/w_{tm} curves resemble the theoretical ones shown before notwithstanding the fact that the theoretical values show the induced velocity by a single layer of vortices and the experimental ones may due to the layers of vortices at different radii.

Chapter IV. Analysis of the Propeller SW–1 and the Comparison with the Experiment.

A wooden propeller, SW-1[1], 1 meter in diameter, was subjected to an exhaustive experiment in 3 meters wind tunnel of the Institute. The propeller is shown in Fig. 24. The blade sections were SE-series of the Institute. The aerofoil characteristics of the blade sections were obtained

(1) This is one-four h model of the wooden propeller used on the long range aeroplane of the Institute during its earlier stages of trial flights.

This document is provided by JAXA.

from the experiment made in the same wind tunnel at speed of 40 m/s .

The wind tunnel experiment of the propeller was carried out also in the same tunnel with the aid of a tower type propeller balance as shown in Fig. 25. The torque is not measured directly by the torque balance marked B in the figure, but it was measured by the torque measuring mechanism marked A in Fig. 25. When the torque is transmitted through the mechanism the rod C (Fig. 26) pushes the bellow containing the oil, the pressure of which is read by means of the precision pressure gauge. The scale on the pressure gauge is calibrated beforehand replacing the propeller with a fan brake and measuring the torque by the torque balance B. In this case there is no need of paying attention to the perfect parallelism of the thrust line of the propeller and the knife edge axis, nor to the agreement of the thrust line and the direction of the wind which introduces considerable error in torque measurement in case of a propeller. As for the experiment of blade sections, the results obtained were converted to the case of two dimensional flow using the conversion formulae for rectangular aerofoil.

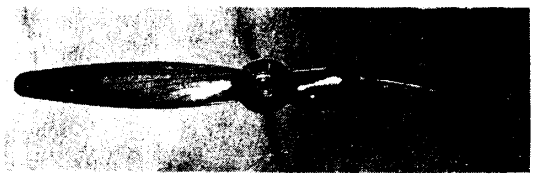

Fig. 24.

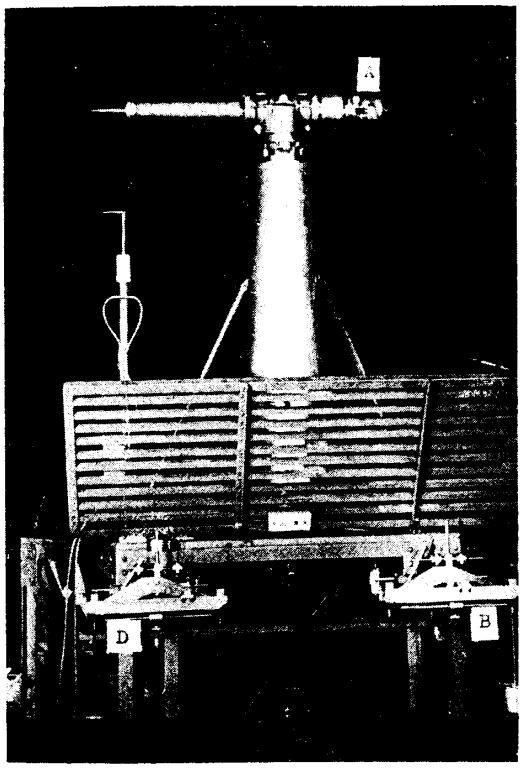

Fig. 25.

This document is provided by JAXA.

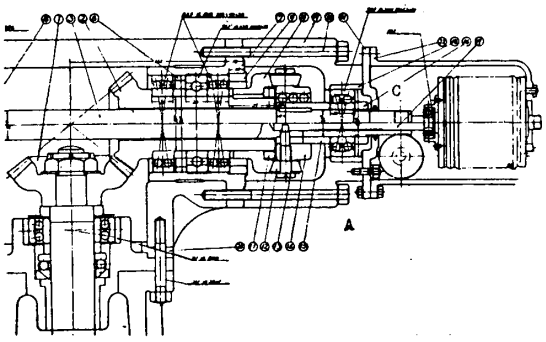

Fig. 26.

The aerofoil characteristics thus obtained are given in Table 16.

TABLE 16.

Thickness ratio	No-lift angle δ	k	C_{zmax}
10 %	-4·7°	0·86	1·27
12 %	-5·65°	0·855	1·36
14 %	-6·65°	0 84	1·43
16 %	-7·85°	0·805	1·48

where $C_z = 2\pi k \sin(\alpha+\delta)$

The dimensions of the propeller measured on the actual model are as shown in Table 17.

TABLE 17.

r/R	t	k	δ	θ (from chord line)
	m			
0 2	0·125	0·80	-9°	54·3°
0 4	0·117	0·805	-7·8°	34·8°
0·6	0 100	0·85	-6·0°	25·5°
0·75	0·082	0·855	-5·1°	21·1°
0·85	0·068	0·86	-4·85°	19 15°
0·925	0·056	0·86	-4·8°	17·8°
0·975	0·047	0·86	-4·7°	17·1°

(1) The experiments were carried out at 2000 r.p.m. and the Reynolds number for blade section at 0·75 R was about $4\,5\times10^5$ when $v/nD = 0{\cdot}524$. Whereas the experiments of aerofoils were made at Reynolds number of about $8{\cdot}4\times10^5$.

This document is provided by JAXA.

Analysis 1. $\mu_0 = 6$ or $v/nD = 0{\cdot}524$.

In this case we have

TABLE 18.

r/R	α in radian (from no-lift angle)	β
0·2	0·41	1·28
0·4	0·347	1·69
0·6	0·279	1·89
0·75	0·24	2·33
0·85	0·224	2·80
0·925	0·217	3·41
0·975	0·212	4·06

Supposing the section at $r/R = 0{\cdot}05$ is non active we have the following equations to determine the circulation:

$$
\begin{aligned}
2{\cdot}81J_2 - 0{\cdot}35J_3 - 0{\cdot}03J_4 &= 0{\cdot}082,\\
-0{\cdot}28J_2 + 3{\cdot}43J_3 - 0{\cdot}42J_4 - 0{\cdot}02J_5 - 0{\cdot}01J_6 &= 0{\cdot}139,\\
-0{\cdot}01J_2 - 0{\cdot}34J_3 + 3{\cdot}70J_4 - 0{\cdot}35J_5 - 0{\cdot}08J_6 - 0{\cdot}02J_7 &= 0{\cdot}168,\\
-0{\cdot}04J_3 - 1{\cdot}06J_4 + 5{\cdot}68J_5 - 1{\cdot}03J_9 - 0{\cdot}11J_7 - 0{\cdot}05J_8 &= 0{\cdot}180,\\
-0{\cdot}01J_3 - 0{\cdot}15J_4 - 0{\cdot}95J_5 + 6{\cdot}16J_6 - 0{\cdot}79J_7 - 0{\cdot}25J_8 &= 0{\cdot}191,\\
-0{\cdot}06J_4 - 0{\cdot}19J_5 - 2{\cdot}46J_6 + 10{\cdot}02J_7 - 2{\cdot}18J_8 &= 0{\cdot}201,\\
-0{\cdot}03J_4 - 0{\cdot}09J_5 - 0{\cdot}50J_6 - 2{\cdot}12J_7 + 10{\cdot}80J_8 &= 0{\cdot}207,
\end{aligned}
\tag{58}
$$

$$\text{where} \quad J = \frac{p\Gamma}{4\pi vR} = \frac{\Gamma}{2\pi vR} .$$

The simple vortex theory gives immediately

$$
\begin{aligned}
J_2 &= 0{\cdot}0360, & J_6 &= 0{\cdot}0503,\\
J_3 &= 0{\cdot}0517, & J_7 &= 0{\cdot}0456,\\
J_4 &= 0{\cdot}0582, & J_8 &= 0{\cdot}0409.\\
J_5 &= 0{\cdot}0540,
\end{aligned}
$$

This document is provided by JAXA.

From these approximate values we have the following solution o the equations

$$J_2 = 0{\cdot}036\,, \qquad J_6 = 0{\cdot}047\,,$$
$$J_3 = 0{\cdot}051\,, \qquad J_7 = 0{\cdot}039\,,$$
$$J_4 = 0{\cdot}056\,, \qquad J_8 = 0{\cdot}030\,.$$
$$J_5 = 0{\cdot}052\,,$$

We can also easily calculate the induced velocities w_t and w_a at the blade element as follows

TABLE 19.

r/R	$w_t/\omega r$	w_a/v
0·2	0·15	0·216
0·4	0·055	0·318
0·6	0·029	0·372
0·75	0·017	0·348
0·85	0·014	0·354
0·925	0·013	0·408
0·975	0·015	0·510

In order to calculate the contribution of the profile resistance towards the thrust and torque, it is essential to know the effective angle of incidence of the blade elements.

Let α_e = effective angle of incidence,
V_e = effective resultant velocity.

Then we have

$$\Gamma = k\pi t V_e \sin\alpha_e\,. \qquad (59)$$

The effective angle of incidence can be calculated from the above formula and the corresponding values of the coefficients of the profile resistance can be obtained from the data in wind tunnel experiment. We have the following result shown in Table 20.

This document is provided by JAXA.

TABLE 20.

r/R	α_e (from chord line)	C_{xo}
0·2	4·4°	0·015
0·4	4·3°	0·014
0·6	4·1°	0·014
0·75	4·5°	0·013
0·85	4·1°	0·013
0·925	3·8°	0·012
0·975	2·4°	0·012

Now it is easy to calculate the thrust and torque. It proceeds as follows:

We have when the profile resistance of the element is neglected

$$\left(\frac{dT}{dr}\right)_0 = \rho p \Gamma(\omega r - w_t) .$$

Putting

$$\left(\frac{dC_T}{dr}\right)_0 = \frac{1}{\rho n^2 D^4}\left(\frac{dT}{dr}\right)_0, \quad \left(\frac{dC_p}{dr}\right)_0 = \frac{1}{\rho n^3 D^5}\left(\frac{\omega dQ}{dr}\right)_0,$$

$$\left(R\frac{dC_T}{dr}\right)_0 = \frac{\pi^3}{\mu_0} J \frac{r}{R}(1 - w_t/\omega r), \quad \left(R\frac{dC_p}{dr}\right)_0 = \frac{\pi^4}{\mu_0^2} J \frac{r}{R}(1 + w_a/v) . \tag{60}$$

The thrust and torque due to the profile resistance can be calculated by the following formulae

$$\frac{dT_p}{dr} = -\frac{1}{2}\rho p C_{xo} v^2 t \sqrt{1+\mu^2}, \quad \frac{\omega dQ_p}{dr} = \frac{1}{2}\rho p C_{xo} \omega^2 r^2 v t \sqrt{1+\mu_2},$$

$$\left(R\frac{dC_T}{dr}\right)_p = -\frac{p\pi^2 C_{xo}}{8\mu_0^2}\frac{t}{R}\sqrt{1+\mu^2}, \tag{61}$$

$$\left(R\frac{dC_p}{dr}\right)_p = \frac{p\pi^3 C_{xo}}{8\mu_0}\left(\frac{r}{R}\right)^2 \frac{t}{R}\sqrt{1+\mu^2} = \mu_0 \pi \left(\frac{r}{R}\right)^2 \left(R\frac{dC_T}{dr}\right)_p .$$

This document is provided by JAXA.

The values of thrust and torque on the elements of the blade are calculated in Table 21.

TABLE 21.

r/R	$\left(R\frac{dC_T}{dr}\right)_0$	$\left(R\frac{dC_P}{dr}\right)_0$	$\left(R\frac{dC_T}{dr}\right)_p$	$\left(R\frac{dC_P}{dr}\right)_p$	$R\frac{dC_T}{dr}$	$R\frac{dC_P}{dr}$
0·2	0·032	0·024	0·0004	0·0003	0·032	0·024
0·4	0·100	0·073	0·0006	0·0017	0·099	0·074
0·6	0·169	0·124	0·0007	0·0049	0·168	0·129
0·75	0·198	0·142	0·0007	0·0071	0·197	0·149
0·85	0·203	0·146	0·0006	0·0086	0·202	0·155
0·925	0·184	0·137	0·0005	0·0084	0·183	0·145
0·975	0·149	0·119	0·0005	0·0068	0·149	0·126

The total thrust and torque of the propeller can be obtained by the graphical integration of the thrust and torque grading curves.

We have[1]

$$C_T = 0{\cdot}116, \quad C_P = 0{\cdot}089 \quad \text{and} \quad \eta = 0{\cdot}68,$$

While the experiment gives (see Fig. 28)

$$C_T = 0{\cdot}122, \quad C_P = 0{\cdot}092 \quad \text{and} \quad \eta = 0{\cdot}68.$$

In the above calculations it was thought that the induced velocities are small compared with the translational and tangential velocities of the propeller and these induced velocities were neglected in calculating the configuration of the vortices, or in other words when determining the value of μ_0. In the actual case, however, the induced velocities w_a is fairly large compared to v.

Therefore it may be seen that the values of thrust and torque calculated under the assumption of the smallness of the induced velocities would lead to erroneous result. More accurate values can be obtained supposing

(1) The resistance of the boss alone was measured and it was found to be negligibly small.

This document is provided by JAXA.

that the propeller is advancing with the velocity $v+w_a$ and rotating with the tangential velocity $\omega r-w_t$. The values of w_a and w_t are different for each blade element, but for an approximate purpose it is sufficient to choose the values at $r/R=0.75$. In the present case we have

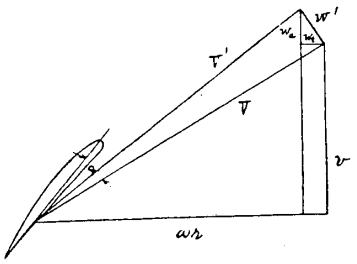

Fig. 27.

$$v+w_a=1.348v\,,\quad \omega r-w_t=0.983\omega r\,,$$

and the new value of μ_0 becomes 4·37.

The fundamental equations (40) become then (see Fig. 27)

$$\Gamma=k\pi tV'(\alpha-w'/V')\,.$$

In this expression the apparent angle of incidence α is not altered and can be calculated by

$$\alpha=\theta-tg^{-1}\frac{v}{\omega r}\,,$$

as before, ignoring the induced velocities.

The values of w' and V' should be now calculated supposing

$$v'=1.348v \quad\text{and}\quad (\omega r)'=0.983\omega r \quad\text{and}$$
$$\mu_0'=4.37.$$

The equations to determine Γ become

$$\begin{aligned}
3.23J_2-0.45J_3-0.06J_4-0.01J_5&=0.112,\\
-0.46J_2+4.29J_3-0.63J_4-0.05J_5-0.04J_6&=0.187,\\
-0.04J_2-0.51J_3+4.83J_4-0.52J_5-0.15J_6-0.03J_7-0.02J_8&=0.226,\\
-0.01J_2-0.08J_3-1.52J_4+7.59J_5-1.46J_7-0.17J_7-0.09J_8&=0.243,\\
-0.03J_3-0.27J_4-1.34J_5+8.35J_6-1.17J_7-0.36J_8&=0.258,\\
-0.01J_3-0.12J_4-0.30J_5-3.40J_6+13.58J_7-2.99J_8&=0.271,\\
-0.07J_4-0.15J_5-0.75J_6-2.90J_7+14.61J_8&=0.279.
\end{aligned}\tag{62}$$

This document is provided by JAXA.

where $J = \frac{p\Gamma}{4\pi vR}$ as before.

Solving these equations we have the following result.

TABLE 22.

r/R	J	$w_t/\omega r$	w_a/v	$R\frac{dC_T}{dr}$	$R\frac{dC_P}{dr}$
0·2	0·044	0·25	0·19	0·034	0·029
0·4	0·057	0·088	0·27	0·106	0·080
0·6	0·061	0.045	0·31	0·179	0·134
0·75	0·055	0·028	0·30	0·206	0·152
0·85	0·049	0·023	0·32	0·209	0·157
0·925	0·041	0·021	0·35	0·191	0·146
0·975	0·031	0·026	0·47	0·152	0·127

The graphical integration gives

$$C_T = 0{\cdot}122\,, \quad C_T = 0{\cdot}093\,, \quad \eta = 0{\cdot}69\,.$$

This is in very good agreement with the experiment.

We can also see that there is no need of proceeding to the further approximation. The new value of μ_0 becomes 4·49. This is not so different from 4·37 as does 4·37 from 6.

Analysis 2. $\mu_0 = 4{\cdot}37$ or $v/nD = 0{\cdot}719$.

The equations to determine the circulation become now

$$\begin{aligned}
3{\cdot}23J_2 - 0{\cdot}45J_3 - 0{\cdot}06J_4 - 0{\cdot}01J_5 &= 0{\cdot}051,\\
-0{\cdot}46J_2 + 4{\cdot}29J_3 - 0{\cdot}63J_4 - 0{\cdot}05J_5 - 0{\cdot}04J_6 &= 0{\cdot}089,\\
-0{\cdot}04J_2 - 0{\cdot}51J_3 + 4{\cdot}83J_4 - 0{\cdot}52J_5 - 0{\cdot}15J_6 - 0{\cdot}03J_7 - 0{\cdot}02J_8 &= 0{\cdot}111,\\
-0{\cdot}01J_2 - 0{\cdot}08J_3 - 1{\cdot}52J_4 + 7{\cdot}59J_5 - 1{\cdot}46J_6 - 0{\cdot}17J_7 - 0{\cdot}09J_8 &= 0{\cdot}127,\\
-0{\cdot}03J_3 - 0{\cdot}27J_4 - 1{\cdot}34J_5 + 8{\cdot}35J_6 - 1{\cdot}17J_7 - 0{\cdot}36J_8 &= 0{\cdot}134,\\
-0{\cdot}01J_3 - 0{\cdot}12J_4 - 0{\cdot}30J_5 - 3{\cdot}40J_6 + 13{\cdot}58J_7 - 2{\cdot}99J_8 &= 0{\cdot}141,\\
-0{\cdot}07J_4 - 0{\cdot}15J_5 - 0{\cdot}75J_6 - 2{\cdot}90J_7 + 14{\cdot}61J_8 &= 0{\cdot}146,
\end{aligned} \tag{63}$$

where $J = \frac{p\Gamma}{4\pi vR}$.

This document is provided by JAXA.

The solution of these equations gives the following result.

TABLE 23.

r/R	J	$w_t/\omega r$	w_a/v	$R\frac{dC_T}{dr}$	$R\frac{dC_P}{dr}$
0·2	0·020	0·114	0·092	0·025	0·022
0·4	0·028	0·043	0·131	0·075	0·066
0·6	0·030	0·022	0·153	0·124	0·112
0·75	0·029	0·015	0·168	0·151	0·131
0·85	0·025	0·013	0·175	0·148	0·132
0·925	0·021	0·013	0·210	0·135	0·127
0·975	0·016	0·014	0·253	0·108	0·107

The graphical integration gives

$$C_T = 0{\cdot}086\,, \quad C_P = 0{\cdot}077\,, \quad \eta = 0{\cdot}804\,,$$

Proceeding to the second approximation as before, we have

$$\mu_0' = 3{\cdot}70\,.$$

The calculation gives finally

$$C_T = 0{\cdot}089\,, \quad C_P = 0{\cdot}079\,, \quad \eta = 0{\cdot}81\,.$$

The experiment gives in this case

$$C_T = 0{\cdot}089\,, \quad C_P = 0{\cdot}0795\,, \quad \eta = 0{\cdot}80\,.$$

Analysis. 3. $\mu_0 = 3$, or $v/nD = 1{\cdot}047$.

The equations to determine the circulation become

$$\begin{aligned}
&3{\cdot}63J_2 - 0{\cdot}55J_3 - 0{\cdot}08J_4 - 0.01J_5 - 0{\cdot}01J_6 = 0{\cdot}007,\\
&-0{\cdot}64J_2 + 5{\cdot}42J_3 - 0{\cdot}85J_4 - 0{\cdot}09J_5 - 0{\cdot}04J_6 - 0{\cdot}01J_7 - 0{\cdot}01J_8 = 0{\cdot}019,\\
&-0{\cdot}07J_2 - 0{\cdot}76J_3 + 6{\cdot}44J_4 - 0{\cdot}74J_5 - 0{\cdot}23J_6 - 0{\cdot}05J_7 - 0{\cdot}05J_8 = 0{\cdot}026,\\
&-0{\cdot}03J_2 - 0{\cdot}14J_3 - 2{\cdot}21J_4 + 10{\cdot}50J_5 - 2{\cdot}07J_6 - 0{\cdot}25J_7 - 0{\cdot}15J_8 = 0{\cdot}030,\\
&-0{\cdot}01J_2 - 0{\cdot}07J_3 - 0{\cdot}43J_4 - 1{\cdot}95J_5 + 11{\cdot}57J_6 - 1{\cdot}58J_7 - 0{\cdot}52J_8 = 0{\cdot}040,\\
&-0{\cdot}01J_2 - 0{\cdot}03J_3 - 0{\cdot}21J_4 - 0{\cdot}46J_5 - 4{\cdot}84J_6 + 19{\cdot}09J_7 - 4{\cdot}25J_8 = 0{\cdot}045,\\
&-0{\cdot}01J_2 - 0{\cdot}02J_3 - 0{\cdot}13J_4 - 0{\cdot}25J_5 - 1{\cdot}10J_6 - 4{\cdot}09J_7 + 20{\cdot}45J_8 = 0{\cdot}051,
\end{aligned} \tag{64}$$

where $J = \dfrac{p\Gamma}{4\pi v R}$.

This document is provided by JAXA.

The solution of these equations gives the results shown in Table 24.

TABLE 24.

r/R	J	$w_t/\omega r$	w_a/v	$R\frac{dC_T}{dr}$	$R\frac{dC_P}{dr}$
0·2	0·002	0·0008	0·0029	0·003	0·003
0·4	0·0048	0·0016	0·0023	0·018	0·023
0·6	0·0055	0·0018	0·0059	0·032	0·041
0·75	0·0052	0·0018	0·0088	0·040	0·051
0·85	0·0054	0·0018	0·0117	0·046	0·058
0·925	0·0048	0·0016	0·0112	0·045	0·057
0·975	0·0038	0·0013	0·0112	0·037	0·049

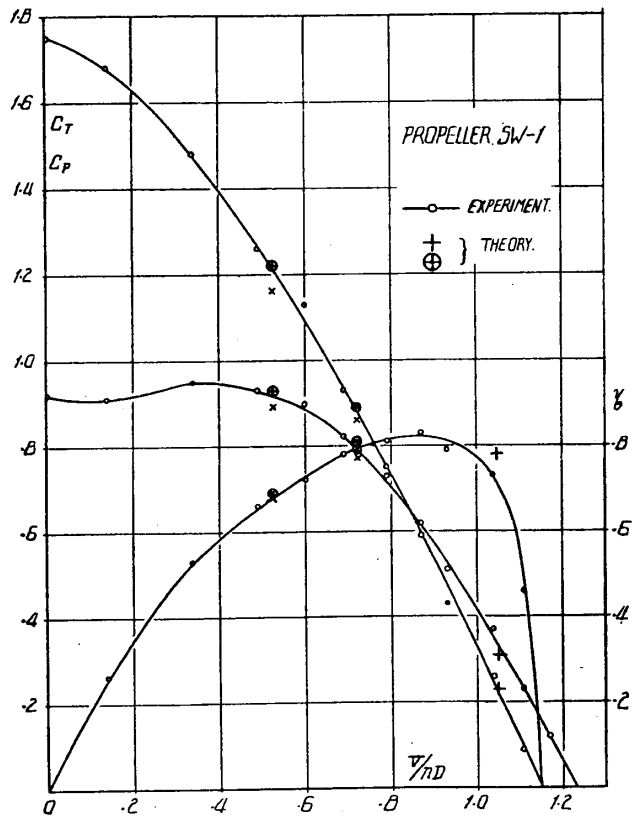

Fig. 28.

Graphical integration gives

$C_T = 0{\cdot}023$, $C_P = 0{\cdot}031$,

$\eta = 0{\cdot}78$.

From the smallness of the induced velocities, it may be seen that the second approximation is not necessary in this case.

The experiment gives[1]

$C_T = 0{\cdot}022$, $C_P = 0{\cdot}032$,

$\eta = 0{\cdot}72$.

In Fig. 28 the theoretical values obtained from the first and second approximation are shown respectively by × and ⊗.

(1) In this case the effect of the boss may be more pronounced than in former cases and the discrepancy between the theory and the experiment may perhaps due to the neglect of the resistance of the boss.

This document is provided by JAXA.

Author's thanks are due to Prof. K. Wada, Director of the Institute, for having given him valuable advices during the preparation of this paper, and to Messrs. Yosida, Hirooka and Takahashi for having assisted him in carrying out the experiments and in numerical calculations.

Conclusion.

1. The consideration of the finiteness of the number of blades in propeller theory is not insurmontably difficult as might at first appears, at least for practical applications.

2. The tip effect of the propeller is widely different according to the blade form, pitch angle etc. and it may be as great as 14 percent even for low pitched propeller in thrut estimation.

5. The distribution of the instantaneous velocity in the wake can be calculated theoretically.

4. The performance of a propeller, which takes the tip effect into consideration, computed by the present method, affords complete agreement with the experiment.

5. It seems to the author that the performance of a propeller can be computed theoretically in an accurate manner from the characteristics of the blade elements only.

This document is provided by JAXA.

Appendix.

Aerofoil Characteristics of Blade Sections of the Propeller analysed in Chapter IV.

Five rectangular aerofoils of aspect ratio 5 were tested in 3 m wind tunnel of the Institute. The chord was 30 cm. and the wind speed was about 40 m/s. Therefore the Reynolds number

$$R_e = vt/\nu \quad (v = \text{velocity}, \; t = \text{chord}).$$

was about $8{\cdot}4 \times 10^5$.

Fig. 29.

The 14 percent thickness ratio aerofoil is shown in Fig. 29 as an example. The other aerofoils are similar to this, differing only in the

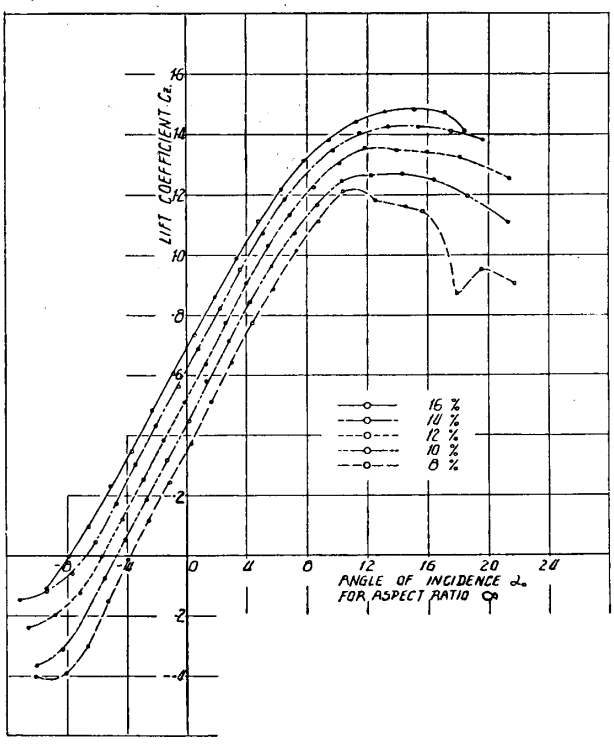

Fig. 30 (a).

This document is provided by JAXA.

thickness ratio. The results of the experiment were converted to C_z and C_x corresponding to infinite aspect ratio making use of the following convertion formulae:

$$\Delta\alpha = \frac{C_z}{\pi\lambda}(1+0{\cdot}154) \quad \text{radians},$$
$$C_{xi} = \frac{C_z^2}{\pi\lambda}(1+0{\cdot}041), \tag{65}$$

where λ = aspect ratio.

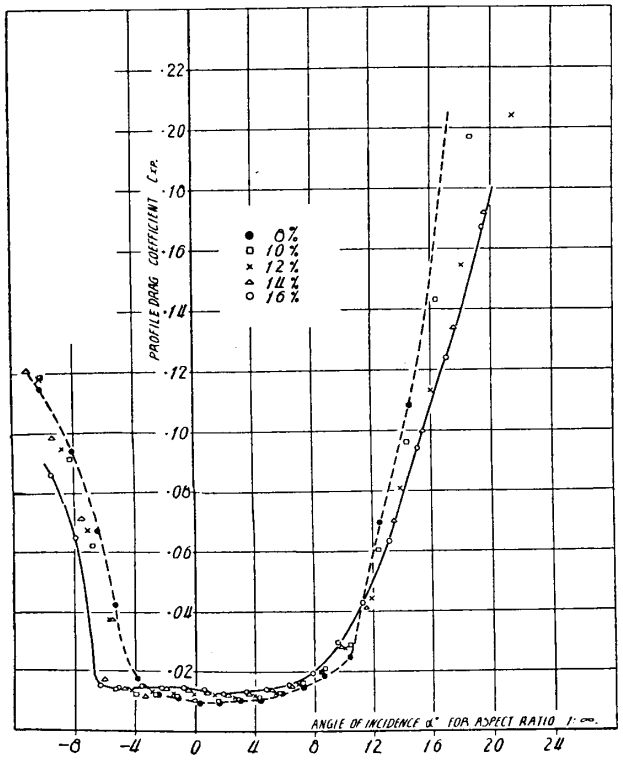

Fig. 30 (b).

The results are shown in Fig. 30.

This document is provided by JAXA.